Seasonal variation of mercury concentration of ancient olive groves of Lebanon.

Nagham Tabaja[1,2,3], David Amouroux[4], Lamis Chalak[2], François Fourel [5], Emmanuel Tessier [4], Ihab Jomaa [6], Milad El Riachy [7], Ilham Bentaleb [1]

[1] ISEM, Univ Montpellier, CNRS, IRD, Montpellier, France
[2] Faculty of Agronomy, Plant Production Department, The Lebanese University, Dekwaneh, Lebanon
[3] Plateforme de Recherche et d'Analyses en Sciences de l'Environnement (PRASE), Ecole Doctorale de Sciences et Technologie, Université Libanaise, Hadath, Liban
[4] Université de Pau et des Pays de l'Adour, E2S/UPPA, CNRS, Institut des Sciences Analytiques et de Physico-Chimie pour l'Environnement et les Matériaux (IPREM), PAU, France
[5] UMR CNRS 5023 LEHNA, Université Claude Bernard Lyon 1, Villeubanne, France
[6] Department of Irrigation and Agrometeorology, Lebanese Agricultural Research Institute (LARI), P.O. box 287, Zahle, Lebanon
[7] Department of Olive and Olive Oil, Lebanese Agricultural Research Institute (LARI), P.O. box 287, Zahle, Lebanon

Correspondence to: Ilham Bentaleb (Email: ilham.bentaleb@umontpellier.fr, Tel: +33(0) 6 38 61 57 69)

Abstract. This study aimed to investigate the seasonality of the mercury (Hg) concentration of olive trees foliage, an iconic tree of the Mediterranean basin. Hg concentrations of foliage, stems, soil surface, and litter were analyzed on monthly basis in ancient olive trees growing in two groves in Lebanon, Bchaaleh and Kawkaba (1300 and 672 m.a.s.l respectively). A significantly lower concentration was registered in stems (~7-9 ng/g) with respect to foliage (~35-48 ng/g) in both sites with the highest foliage Hg concentration in late winter-early spring and the lowest in summer. It is noteworthy that olive fruits also have low Hg concentration (~7-11 ng/g). The soil has the highest Hg content (~62-129 ng/g) likely inherited through the cumulated litter biomass (~ 63-76 ng/g). A good covariation observed between our foliage Hg time-series analysis and those of ~~pCO₂ and~~ atmospheric Hg concentrations ~~of the atmospheri Northern hemisphere~~ available for southern Italy in the western Mediterranean basin confirms that mercury pollution can be studied through olive trees. More precisely, spring sampling is recommended if the objective is to assess the tree's susceptibility to Hg uptake. ~~This may draw an adequate baseline for global inventories~~ Our study draws an adequate baseline for Eastern Mediterranean and region with similar climate inventories on Hg vegetation uptake and new studies on olive trees in the Mediterranean to reconstruct regional Hg pollution concentrations in the past and present.

Keywords: Eastern Mediterranean, ancient groves, *Olea europaea* L., mercury pollution, plant tissues, soil and litter

Introduction

Mercury (Hg) is among the most widely distributed potentially toxic metals polluting the Earth (Briffa et al. 2020). It is found as all heavy metals naturally on the Earth's crust reservoir and in the atmosphere through the natural long-term Hg biogeochemical cycle (i.e., volcanic activities, geological weathering). This metal is easily modified into several oxidation states and it can also be spread through many ecosystems (Boening 2000). The natural Hg cycle has been modified due to anthropogenic activities (i.e., mining, smelting, soil erosion due to deforestation, gold extraction, agriculture-fertilizers, manure) (Patra and Sharma 2000). Among natural and anthropogenic Hg emissions, inorganic elemental Hg (Hg(0)) is the most dominant chemical form (Clarkson and Magos 2006). It is generally transferred through the atmosphere by the winds and mass air. It is primarily transferred through the atmosphere by air mass movement and can undergo long-range transport. Because of its high volatility and susceptibility to oxidation, elemental Hg(0) is the predominant form of Hg in the atmosphere that can be accumulated into foliage. This highly diffusive Hg can easily pass biological barriers (i.e. cell membranes, foliage, skin). Mercury has three oxidation states, namely, Hg(0) (elemental mercury), Hg(I) (mercurous), or Hg(II) (mercuric), although Hg(I) mercurous form is not stable under typical environmental conditions and, therefore, is rarely observed. It is likely that the Hg(II) high binding affinities bind covalently with organic groups to form the widespread toxic methylmercury (MeHg, CH3Hg+) (Du and Fang, 1983; Clarkson and Magos 2006; Pleijel et al., 2021). Anthropogenic activities stimulate an accumulation of heavy metals in terrestrial and aquatic ecosystems. This can remain for over 100 years after the closure of the pollution source. The exchange of Hg between the soil and plants is not stable and is variable dependent (e.g. cation-exchange capacity, soil pH, soil aeration, and plant species) (Patra and Sharma 2000).

Large forests with large foliage surface area Forests are known to act as a sink of atmospheric Hg in the ecosystem. Plant foliage takes up of Hg deposited on leaf surfaces through the stomata (i.e. Photosynthesis Leaf gas exchange) and leaf cuticles (Hanson et al. 1995; Jiskra et al. 2018; Li et al. 2017; Lodenius et al. 2003; Maillard et al. 2016; Rea et al. 2002; Yanai et al. 2020) where it accumulates with minimal mobility and small portions released back into the atmosphere or transfers the Hg transferred through the to other plant organs (Cavallini et al. 1999; Hanson et al. 1995; Li et al. 2017; Lodenius et al. 2003; Schwesig and Krebs 2003). All together these authors contributed to highlight the dynamic role of the foliar surfaces in terrestrial forest landscapes acting as a source or sink dependent on the magnitude of current Hg concentrations. Hanson et al. (1995) suggested a species-specific compensation concentrations (or compensation points) for Hg deposition. These two Hg absorption pathways in plants are also described in Hg contaminated sites on several plant species reporting the accumulation of Hg in the foliage and also in the roots where Hg can be absorbed through xylem sap (Assad et al. 2017). Tree's Hg is transferred to the forest floor through litter and throughfall and hence passes to the soil (Rea et al. 1996). Litter is said to constitute 30 to 60 % of the Hg atmospheric deposition in Europe and North America forests (Rea et al. 1996; Blackwell and Driscoll 2015; Zhou et al. 2018). The Hg input through the litter is greater than the input from that of the wet deposition (Wang et al., 2016). The Litter Hg is the dominant pathway in forests where it contributes to and 90 % of the dry deposition to the forest (Wright et al., 2016).

Hg is redistributed to the forest floor through litter and throughfall and hence passes to the soil (Rea et al. 1996). The Hg input through the litter is greater than the input from that of the wet deposition (Wang et al., 2016). Litter has been

74 estimated to constitute 30 to 60 % of the Hg atmospheric deposition in Europe and North America forests (Rea et al.

75 1996; Blackwell and Driscoll 2015; Zhou et al. 2018). According to Wright et al., (2016) the litter Hg is the dominant

76 pathway in forests where it contributes 53 to 90 % of the dry deposition to the forest. ~~(Wright et al., 2016)~~.

77 In ~~earth~~ terrestrial ecosystem, soil as part of the geological reservoir has naturally the highest Hg reservoir (Obrist et

78 al., 2018; O'Connor et al., 2019) followed by trees (Yang et al., 2018). This Hg is provided by natural geological

79 sources and natural events such as forest fires, volcanic eruptions (Ermolin et al. 2018; Obrist et al. 2018; O'Connor

80 et al. 2019) and anthropogenic sources (UNEP, 2019). ~~In return, soil and plants can reemit Hg to the atmosphere~~

81 ~~through diffusion and transpiration during photo-respiration biological processes (Luo et al., 2016; Yang et al., 2018a;~~

82 ~~Assad, 2017; Schneider et al., 2019; Gworek et al., 2020). Trees are hence important drivers of Hg between the~~

83 ~~atmosphere and the soil (Yang et al. 2018) .~~

84 Though variable from year to year, Hg emission to the atmosphere from biomass burning is considered as an important

85 driver of the global Hg biogeochemical cycle (Friedli et al., 2009; De Simone et al., 2015; McLagan et al., 2021;

86 Dastoor et al., 2022). Soil can also release Hg to the atmosphere (Luo et al., 2016; Assad, 2017; Yang et al., 2018;

87 Schneider et al., 2019; Gworek et al., 2020; Pleijel et al., 2021) and also behave as a source of Hg to the plants. Hg of

88 the soil is is taken up by the roots along with the water , it is translocated to other parts (ie. Stems, Leaves) of the plant

89 using the xylem sap (Bishop et al., 1998; Li et al., 2017). This pathway have been described on several plant species

90 in Hg contaminated sites (Assad et al. 2017). Trees are hence considered as important drivers of Hg exchange between

91 the atmosphere and the soil (Yang et al. 2018). The recent studies on Hg uptake by vegetation have highlighted the

92 importance of the role of different parameters as vapor pressure deficit, soil water content, climatic conditions, date

93 of sampling, leaf mass area, tree functional groups, stomatal conductance, affecting potentially the root uptake of Hg

94 dissolved in soil water and the absorption rate via stomata and eventually the Hg leaf content (Rea et al., 2002; Obrist

95 et al., 2011; Blackwell & Driscoll, 2015; Yang et al., 2018; Wohlgemuth et al., 2021). In polluted sites the soil is the

96 main source of Hg to the vegetation while away from those sites the atmosphere is the most important source (Naharro

97 et al., 2018). The Hg source in foliage varies with respect to the amount of contamination (Hanson et al., 1995).

98 The studies of the Hg cycle in forest ecosystems show that gaseous elemental Hg(0) is the main source taken up by

99 plants (Bishop et al. 2020; Zhou et al. 2021). ~~Differences are observed between ecological functional traits and species~~

100 ~~among other factors. Hg in tree rings is also analyzed usually to determine if the Hg concentration are influenced more~~

101 ~~by the soil Hg concentration or by the atmospheric Hg deposition. This atmospheric deposition that has declined in~~

102 ~~recent decades can be shown in the declining concentration from the older to newer tree rings suggesting a more~~

103 ~~important uptake through the foliage than the roots. Hg dendrochemistry can help investigate Hg past impacts on~~

104 ~~terrestrial ecosystems and also help predict future changes in the cycle of Hg in forests (Yanai et al., 2020). The recent~~

105 ~~studies on Hg uptake by vegetation have highlighted the importance of the role of different parameters as vapor~~

106 ~~pressure deficit, soil water content, climatic conditions, date of sampling, leaf mass area, tree functional groups,~~

107 ~~stomatal conductance affecting potentially the root uptake of Hg dissolved in soil water and the absorption rate via~~

108 ~~stomata and eventually the Hg leaf content (Blackwell & Driscoll, 2015; Rea et al., 2002; Wohlgemuth et al., 2021;~~

109 ~~Yang et al., 2018).~~ Analysis of long term atmospheric Hg(0) and CO_2 concentrations are very informative to

110 understand the role of the vegetation in the global Hg cycle (Jiskra et al., 2018). Emission reduction measures adopted

in Europe and North America since the 70s are corroborated by Hg dendrochemistry analysis showing a declining Hg concentration trend from the older to newer tree rings. Indeed, tree ring Hg (dendrochronology) is a powerful archiving tool for atmospheric Hg(0). After Hg(0) oxidation inside the leaves, Hg(II) bind to organic compounds and then is transported to the bole wood via the phloem (Beauford et al., 1977; Lindberg et al., 1979). This is corroborated by the recent study of McLagan et al., (2022) showing the benefit of the stable Hg isotope analysis on dendrochemistry. Several studies have evidenced seasonal variations of the atmospheric Hg(0) contents (ie. in temperate Northern Hemisphere by Jiskra et al., 2018; in Western Mediterranean Basin in South Italy (Martino et al. 2022) with high values in winter and low values in summer. Interinstingly, Jiskra et al., (2018) show also a significant positive correlation between the monthly Hg(0) and CO_2 concentrations. They highlighted a one-month offset in Hg(0) summer time minima happening in September in comparison to the CO_2 minima value occurring in August, this trend is not observed in winter time. The uptake of Hg(0) by the vegetation continues during CO_2 respiration periods during the fall and night when the ecosystem exchange of CO_2 turns from being a sink to becoming a source (Wofsy et al., 1993; Jiskra et al., 2018).

The total gaseous Hg (TGM) in the Mediterranean atmosphere is similar to Northern Europe (1.3 to 2.4 ng m^{-3}) (Kotnik et al. 2014). In the case of a semi-closed sea such as the Mediterranean basin with warm summers, high sea-water evaporation, solar radiations and Hg anthropogenic sources, the Mediterranean Sea acts as a net source of Hg to the global atmosphere (Kotnik et al. 2014) making the Mediterranean an air-pollution emission area (Baayoun et al. 2019; Borjac et al. 2019).

The olive tree (*Olea europaea* L.) is one of the most distinctive Mediterranean agro-ecosystems tree species (Besnard et al., 2013), and is adapted to drought (Sghaier et al. 2019). Considered to be among the oldest trees in the Mediterranean basin, centennial olive trees are still growing in many countries along both the eastern and western shore, surviving numerous stresses and are of considerable historical, cultural and ecological importance (Terral et al. 2004). The olive tree still remains a key component of agriculture today and will be into the future. Therefore, it is important to understand the on-site behavior of the olive tree to Hg pollution in its natural Mediterranean growing environment. The Hg source in foliage varies with respect to the amount of contamination. In polluted sites the soil is the main source of Hg while away from those sites the atmosphere is the most important source (Naharro et al. 2018). Therefore, genetic characterization of olive varieties and genetic resources (Khadari et al., 2019; Galatali et al., 2021), description based on morphological characters and phenology of growth stages of olive trees (Sanz-Cortés et al., 2002), experimentation through field irrigation and/or more rarely through drought stress treatments (Alcaras et al., 2016) have been conducted to avoid genetic erosion, optimize the water use for irrigation and hence improve orchard management, and solely to better understand the biodiversity. Only few studies have focused on the response of the olive tree to Hg pollution in its natural Mediterranean environment (Higueras et al., 2012; Higueras et al., 2016; Guarino et al., 2021; Labdaoui et al., 2021).

Lebanon, a small country at the Eastern Mediterranean, is facing important anthropogenic pressure within a changing environment (Gérard and Nehmé 2020). The air quality in Lebanon all over the country is noted to be moderately unsafe with an annual mean concentration of 31 μg/m^3 of PM2.5 (Particulate Matter) which is above the maximum recommended value (10 μg/m^3) (Lebanon: Air Pollution IAMAT 2020). Adding to that, soil samples collected from

different areas in southern Lebanon showed values of Hg concentration ranging between 160-6480 ng/g showing a high contamination levels (Borjac et al. 2020) as indicated by World reference Senesil et al., 1999; Kabata-Pendias & Pendias, 2000. The main contributors of the air pollution include cement industries, mineral and chemical factories, vehicles emissions, food processing and oil refining. Ancient olive groves are found across different agroclimatic areas at different altitudinal belts, still producing olives and oil for consumption with these various pollution pressures. ~~In this study, remote sites were investigated for possible Hg contamination that is expected to be very low, since the atmospheric Hg is still deposited in remote areas (Grigal, 2003). This is due to the surrounding polluted sites and the transfer of pollution through wind and the Mediterranean Sea to other areas. In addition to the lack and scarcity of studies on Hg pollution in the Eastern Mediterranean. The aim was to follow monthly concentrations variation of Hg during two consecutive years 2019-20 in the foliage and stems of olive trees, soils and litter of two ancient groves of Lebanon known to be over 1400 years old (Yazbeck et al., 2018). Specifically, two main objectives are taken into account: 1) How does Hg content vary seasonally in uncontaminated and remote sites? 2) Is Hg uptake from the soil to the foliage low in uncontaminated sites?~~

In this study two sites, known for their century-old olive groves and located at two different altitudes in Lebanon, were selected to assess the Hg contents. In these remote areas, no direct sources of mercury contamination are reported and hence we expect very low Hg concentrations. However, due to atmospheric transport of Hg, dry or wet deposition of Hg can be expected in remote areas (Grigal, 2003). The main objectives of this study are to examine and compare Hg levels in foliage, stems, fruits, litter and soil measured in each of these two olive groves, which we monitored monthly for 18 months. The second objective is to analyze the relative importance of Hg uptake by the soil and foliage in comparison with the atmospheric Hg. Since the distribution of Hg pollution is by nature geographically widespread, and given the extent of Hg pollution in the Mediterranean and the transfer of pollution by wind and the Mediterranean Sea, long-distance contamination occurs over large areas. This study may draw an adequate baseline for Eastern Mediterranean and region of similar climates inventories on Hg vegetation uptake and new studies on olive trees in the Mediterranean to reconstruct regional Hg pollution concentrations in the past and present.

2. Materials and methods

Two monumental olive groves were chosen in the context of their historical and agricultural importance, since these two sites are considered to contain olive trees more than 1400 years old and are still productive.

2.1. Geographic setting and environmental context

2.1.1. Bchaaleh site - North Lebanon

This grove is situated in Batroun district (Latitude 34°12'06'' N, Longitude 35º49'23'' E, Altitude 1300 m.a.s.l.) (Figure 1). Olive trees are growing rainfed in a sandy loam texture soil of grain size analysis of sand, silt and clay percentages are 52.8 %, 38.7 % and 10.7 % respectively. Soil pH is 7.07 ± 0.26 with organic matter and calcium carbonate contents are 1.7 % and 38.3 % respectively (Yazbeck et al. 2018). In this study, soil profiles of carbon and nitrogen contents were analyzed. Organic carbon contents decreased with soil depth from about 4 % at 0-1 cm (Soil

186 surface) to 2.7 % at 30-60 cm. The total nitrogen is about 0.3 % at 1cm depth and 0.2 % at 30-60 cm depth. The olive

187 trees are located on two terraces. The first terrace is at 1.5 meter above the road level while the second is at the road

188 level. They are maintained by the municipality for the last four decades as an endowment property. Precipitation

189 average ranges between 229 and 392 mm in winter and between zero and less than 2 mm/season in summer, while

190 average temperature is between 4 and 8 °C in winter and between 20 and 23 °C in summer and average relative

191 humidity of 63% (data extracted from LARI climatic data) (Table S1, Figure S1).

192 The village is at about 36 km from Chekka town located at a lower altitude (0-200 m.a.s.l.) nearby the sea (Figure 1),

193 and which is classified as a source of air pollution (EJOLT 2019). Chekka is the site of an important national cement

194 factory responsible of carbon dioxide, sulfur dioxide, nitrous oxides, carbon monoxide and particulate material

195 emissions causing respiratory and health issues (Kobrossi et al. 2002) and water pollution (Nassif et al. 2016). At 28

196 km from Bchaaleh, the small commercial port of Selaata (0-37 m.a.s.l.) emits many pollutants (ie. Phosphogypssum,

197 heavy metals, radionuclides) expanding via water and air pathways (Petrlik et al. 2013; Yammine et al. 2010). To our

198 knowledge no direct Hg pollution is reported at Chekka and Selaata sites. However a dissolved gaseous Hg from

199 natural and human activities is saturated in the upper Eastern Mediterranean Sea, Gårdfeldt et al., (2003) have

200 evidenced that Mediterranean Sea is a source of airborne elemental Hg.

201

202
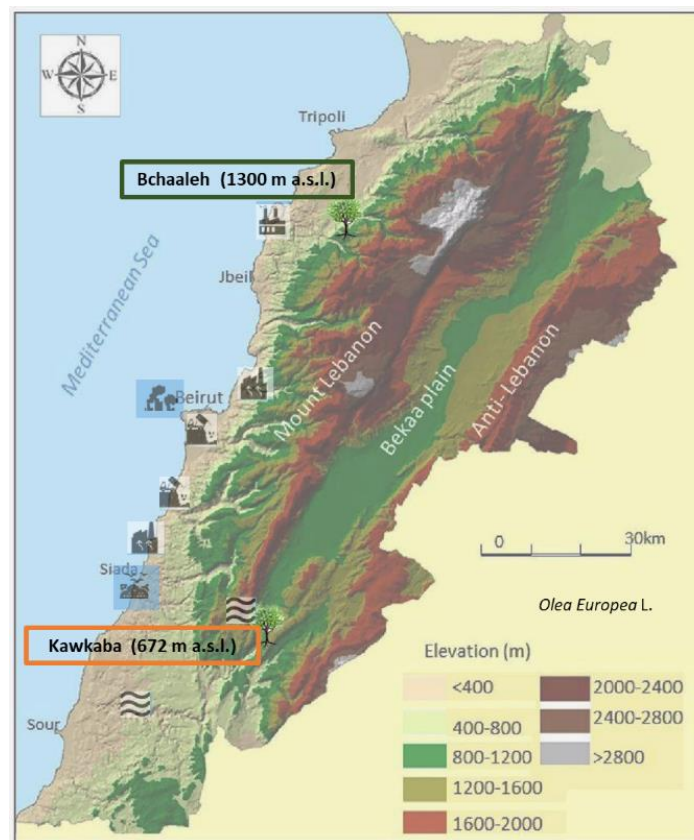
203 **Figure 1.** Site locations of the two selected focus areas (modified after Shared Water Resources of Lebanon, Nova
204 Science Publishers 2017).

205

2.1.2. Kawkaba site - South Lebanon

The second grove is located in the village of Kawkaba, South Lebanon (Latitude 33°23'856'' N, Longitude 35°38'588'' E, Altitude 672 m.a.s.l. (Figure 1). Kawkaba soil is characterized as clay loam soil of pH 7.5 ± 0.5. Soil organic material and calcium carbonate average are 1.7 % and 59.0 % respectively (Al-Zubaidi et al., 2008) and grain size analysis of sand, silt and clay percentages are 6 %, 28 % and 66 % respectively. The analysis of organic carbon and nitrogen at the 0-1 cm and at 0-30 cm decrease from about 9.0 % to 2.2 % and from 0.9 % to 0.3 % for the carbon and nitrogen respectively. Average precipitation ranges between 215 and 374 mm in winter and drop to almost zero mm in summer, while average temperature is between 7 and 11 °C in winter and between 21 and 27 °C in summer and relative humidity of 61% (data extracted from LARI climatic data) (Table S1, Figure S1).

The village has to its east the Hasbani river, originated from the north-western slopes of Mount Hermon in Hasbaya (36 km away from Kawkaba and located at 750 m.a.s.l.) (Badr et al. 2014; Jurdi et al. 2002). On the other hand, the Litani River (170 km long and located at 800 to 1000 m.a.s.l) (Figure 1) rising in the south of the Bekaa valley is about 29 km away from Kawkaba (Abou Habib et al. 2015, Khatib et al. 2018). These two rivers are polluted and for these reasons they are not used for irrigating crops in Kawkaba and surrounding areas while the olive trees are growing rainfed as per indicated by the municipality of Kawkaba. Here as well, we did not find indication of direct Hg pollution. Climatic data in both Bchaaleh and Kawkaba were collected from meteorological station and manual rain gauge installed in the villages by LARI (Lebanese Agricultural Research Institute). CO_2 data used in this study are from NOAA Global Monitoring Laboratory (https://gml.noaa.gov/webdata/ccgg/trends/co2/co2_trend_gl.txt).

2.2. Field sampling

For the Hg concentration analysis, four olive trees of 8 to 15 m foot circumference (3-5 m in diameter and an average height of 4-6 m) were sampled in each of the two groves from February 2019 to September 2020. Within Bchaaleh two trees were selected from the upper terrace (BCO1-Bchaaleh-Tree 1, BCO4-Bchaaleh-Tree 4) and two other trees were sampled from a lower terrace located 1.5 m below the upper one (BCO9-Bchaaleh-Tree 9, BCO12-Bchaaleh-Tree 12) (Figure S2). In Kawkaba, four trees were selected and sampled (KWO1-Kawkaba-Tree 1, KWO2-Kawkaba-Tree 2, KWO3-Kawkaba- Tree 3, KWO4-Kawkaba-Tree 4). For each olive tree, both sun exposed and shaded foliage and stems (terminal portions of 20 cm) with no evidence of pathogens were randomly taken and merged from the upper, middle, and lower canopy position of the olive trees on a monthly basis using a manual pruner. The phenological growth stages of olive trees described by Sanz-Cortés et al.,(2002) in Spain suggest leaf development from March to November. Hence it should be mentioned that the Hg concentration measured on monthly collected foliage represents an average of Hg accumulated in young foliage (year N of collection where N is equal to 2019 and 2020) and older foliage (N-1 year and N-2 years). Fruits were collected in April 2019. Litter and soil surface were separately collected on the whole top surface area of the olive groves and stored in different paper bags once every four months. In parallel, soil sampling was performed using a bucket auger to a maximum depth of 60 cm. In both sites Bchaaleh and Kawkaba, the soil showed uniform color and texture. Soil cores were fractioned in soil surface (0-1 cm), 0 to 30 cm depth and from 30 to 60 cm depth in order to study the effect and accumulation of Hg concentration

244   on the different depth layers. To avoid contamination, gloves were worn while collecting samples, and the equipment

245   was rinsed with methanol between every sample. A set of 453 samples were collected and stored in paper bags until

246   further preparation for the Hg analysis.

247

248   **2.3. Sample preparation for Hg analysis**

249

250   Collected foliage and stems were rinsed with distilled water and then dried for 48 hours in an oven at a temperature

251   of 50°C at maximum (Demers et al., 2013; Li et al., 2017; Pleijel et al., 2021). This procedure likely eliminate any

252   Hg(0) present in the samples. The dried foliage, stems, litter and olive fruits samples were grinded using an electrical

253   stainless grinding machine with no heating system for 5-10 minutes, while soil samples were prepared with a manual

254   natural agate grinder. All samples were later sieved using an inox stainless-steel 125-micron sieve mesh to collect

255   homogeneous powders for analysis. A total of 150 mg for foliage and soil (50 mg/analysis), and 300 mg of litter and

256   stems (100 mg/analysis) were considered in triplicates for analysis of Hg concentrations.

257

258   **2.4. Analytical method**

259

260   For the Hg elemental analysis, a total of 453 powder samples from foliage, stem, grain, litter and soil were analyzed

261   using an advanced Hg analyzer AMA 254 (Altec) as described elsewhere (Barre et al. 2018; Duval et al. 2020). A

262   known amount of sample (50-100 mg) is weight in a nickel boat, using a 10^{-6} g precision balance. The sample aliquot

263   is first dried at 120°C for 60s and subsequently pyrolyzed at 750°C for 150s, under oxygen flow. The resulting gaseous

264   Hg produced during the sample decomposition is amalgamated on a gold trap and then released to an Atomic

265   Absorption spectrometer after a thermal desorption step at 950°C. The AMA 254 instrument was calibrated through

266   several external matrix-matched calibration procedures using the following certified reference materials: IAEA-456

267   sediment (77 ± 5 ng Hg/g), NIST-1575A pine needles (39,9 ± 0,7 ng Hg/g) and IAEA336 (200 ± 40 ng Hg/g). The

268   QA/QC evaluation of the analytical procedure was completed with a continuous monitoring of the blank's values

269   (Nickel boat Hg background noise), every 15 analyzed samples. The precision of the measurements was assessed

270   through replicated analyses (n=2) of 13 % of the total amount of samples (n=453). Average relative standard deviations

271   of 5 % and 2.5 % are thus associated to the reported Hg concentrations for the 2019 and 2020 samples batches,

272   respectively. The absolute detection limit (ADL) of the analytical technique (AMA 254) was estimated at 0.04 ng Hg.

273   As a consequence, the method detection limit (MDL) for samples analyzed were 0.7 ng Hg/g for soil, litter and foliage

274   and 0.4 ng Hg/g for stem and wood. These MDL were much lower than the measured Hg concentration in the various

275   samples.

276   Susbamples of soil were used for carbon and nitrogen elemental contents (%) analysis. A 2 mg (acid washed soil and

277   bulk soil) of powders were weighed into tin capsules and measured by dry combustion using a Pyrocube Elemental

278   Analyser (EA, Elementar GmbH).

279

280

2.5. Statistical analysis

For the statistical analysis we used the R 4.1.0 program. Our data are not normally distributed, so for the effect of tissue type on Hg concentration, Wilcoxon test was used with the tissue type (foliage and stems) as the main effect. Pearson correlation analysis was used to examine the inter-individual correlation of Hg concentration between the trees. Correlation between Hg concentration of soil surface, litter and foliage was studied using a correlation test. For the seasonal effect (Winter: Mid December till Mid-March, Spring: Mid-March till Mid-June, Summer: Mid-June till Mid-September, Autumn: Mid-September till Mid-December) on Hg concentration, Wilcoxon test was used considering the unequal data available for the different seasons. Finally, the effect of climatic factors (Temperature, precipitation, pCO_2) on Hg accumulation was examined using a Wilcoxon test.

3. Results

3.1. Hg concentrations in plant tissues, litter and soil at Bchaaleh and Kawkaba groves

Hg concentrations measured in the different sampled materials (plant tissues, litter and soil) varied generally according to both tree tissues and groves agroclimatic conditions (Table 1). Hg values in the foliage varied significantly between the two groves (p-value=$1.581*10^{-6}$), where the highest concentration was recorded in Bchaaleh (48.1 ± 10.6 ng/g) *vs.* (35 ± 12.4 ng/g) in Kawkaba. Soil surface also recorded a difference in Hg concentration between Bchaaleh and Kawkaba, with 61.9 ± 20.0 ng/g in Bchaaleh and 128.5 ± 9.4 ng/g in Kawkaba. Soil 0-30 cm samples taken from Bchaaleh and Kawkaba groves, values ranged between 31.8 ± 4.7 ng/g and 70.2 ± 23.4 ng/g respectively. In soil 30-60 cm Hg concentrations recorded 19.5 ± 6.73 ng/g at Bchaaleh. No significant differences were recorded for litter and stems Hg concentrations (p-value= 0.0915 and p-value=0.2215 respectively) between the groves, with litter values of 62.9 ± 17.8 at Bchaaleh and 75.7 ± 20.3 ng/g at Kawkaba *vs.* stem values of 7.9 ± 2.8 ng/g at Bchaaleh and 9.0 ± 4.7 ng/g at Kawkaba. Positive correlations were observed between soil and litter in Bchaaleh (r=0.60) and Kawkaba (r=0.95) though statistically insignificant (p-value= 0.40 and 0.13 respectively).

The comparison between Bchaaleh and Kawkaba soil surface Hg contents showed significant difference between the two groves (p-value=0.04746). We observe the same significant difference when comparing the soil horizon of 0-30 cm of both groves. In descending order of Hg concentrations and considering the different sites, plant tissue, soil and litter samples, the Hg concentrations could be ranked in Bchaaleh, soil surface > litter> foliage > soil 0-30 cm > soil 30-60 cm > stems > fruits; and in Kawkaba, soil surface > litter > soil 0-30 > foliage > soil 30-60 > stems > fruits (Table 1).

Table 1. Overall mean values of Hg concentration (ng/g) of the different studied material in both Bchaaleh and Kawkaba olive groves

Sample material	Bchaaleh (BC)			Kawkaba (KW)		
	Average (ng/g)	SD	N	Average (ng/g)	SD	N
Foliage	48.1	10.6	66	35.0	12.4	67
Stems	7.9	2.8	66	9.0	4.7	67
Litter	62.9	17.8	7	75.7	20.3	6
Soil Surface	61.9	20.0	8	128. 5	9.4	6
Soil 0-30cm	31.8	4.7	6	70.2	23.4	5
Soil 30-60cm	19.5	6.7	5	28.0		1
Fruits	7.0	3.5	3	11.0		1

3.2. Seasonal variation of Hg concentration in plant tissues, litter and soil

Hg concentrations recorded between February 2019 and September 2020 (Table 2) reflected a significant seasonal variation in both sites (p-value$<2.2*10^{-16}$)

In Bchaaleh grove, foliage registered its highest Hg concentration during winter and spring with 61.8 ± 7.6 ng/g and 55.1 ± 12.5 ng/g respectively, and its lowest Hg amount during summer and autumn with 41.5 ± 12.7 ng/g and 44.4 ± 6.2 ng/g, respectively. A seasonal effect on foliage and stems was registered (p-value$<2.2*10^{-16}$; Figure 2a,c). The stems and soil 0-30cm highest values was registered in autumn. Significant differences were found in foliage Hg values between summer and winter (p-value=0.00020), and autumn and winter (p-value= 0.00014). Similarly, stems Hg values varied significantly between spring and winter (p-value=0.030), autumn and winter (p-value=0.047). Litter highest Hg content occur in summer in Bchaaleh olive groves (79.3 ± 26.5 ng/g) and the lowest in winter (48.6 ± 13.3 ng/g) (p-value = 0.2286). Highest Hg contents in the soil surface of Bchaaleh is recorded in summer (84.5 ± 21.2 ng/g).

In Kawkaba, the highest Hg concentrations for foliage and stems were registered in spring with 51.8 ± 4.5 ng/g, 11.7 ± 6.7 ng/g respectively (Table 2, Figure 2b,d). Significant differences were found in foliage Hg values between summer and winter (p-value=0.013), autumn and winter (p-value= 0.00067), autumn and spring (p-value=$1.589*10^{-05}$), spring and winter (p-value= $9.383*10^{-05}$) and spring and summer (p-value=$2.327*10^{-06}$). Similarly, stem Hg values varied significantly between spring and winter (p-value=0.006), spring and summer (p-value=0.0036) and autumn and spring (p-value=0.011). There is no seasonal variation between the litter different seasons for Bchaaleh nor for Kawkaba. Bchaaleh and Kawkaba groves soil surface, 0-30 cm and 30-60cm Hg values varied significantly between seasons, (p-value < 0.05). A seasonal variation is observed in both olive groves especially in the foliage.

Table 2. Seasonal mean Hg concentration (ng/g) and standard deviations of the different studied material in both Bchaaleh and Kawkaba olive groves. Grey color indicated the highest Hg concentration values among the different elements during the different seasons

Hg (ng/g)												
Bchaaleh	**Spring**	**SD**	**N**	**Summer**	**SD**	**N**	**Autumn**	**SD**	**N**	**Winter**	**SD**	**N**
Foliage	55.1	12.5	16	41.5	12.7	24	44.4	6.2	12	61.8	7.6	18
Stems	7.8	3.8	16	7.61	3.9	24	8.3	2.7	12	6.4	2.9	18
Litter	79.3	26.5	3	64.7	4	4	55.5	3.54	2	48.6	13.3	3
Soil Surface	58.3	13	3	84.5	21.2	4	50		1	50.6	23.5	3
0-30cm	33.6	6.2	2	32.2	4.3	2	34.5	7.79	2	27	0.7	3
30-60cm	23.1	9.1	2	20.7	10.32	2	19.6	9.05	2	11		1
Kawkaba	**Spring**	**SD**	**N**	**Summer**	**SD**	**N**	**Autumn**	**SD**	**N**	**Winter**	**SD**	**N**
Foliage	51.8	4.5	16	28	7.2	24	28.5	7.2	16	33.9	5.6	18
Stems	11.7	6.7	16	6.5	1.4	24	7.7	2.1	16	6.9	1.6	18
Litter	90.1	29.3	2	67	24	2	70	1.4	2			
Soil Surface	132	8.5	2	118	4.2	2	135.6	2.2	2			
0-30cm	57.9	11.2	2	65.8		1	84.8	36.4	2			
30-60cm	28		1									
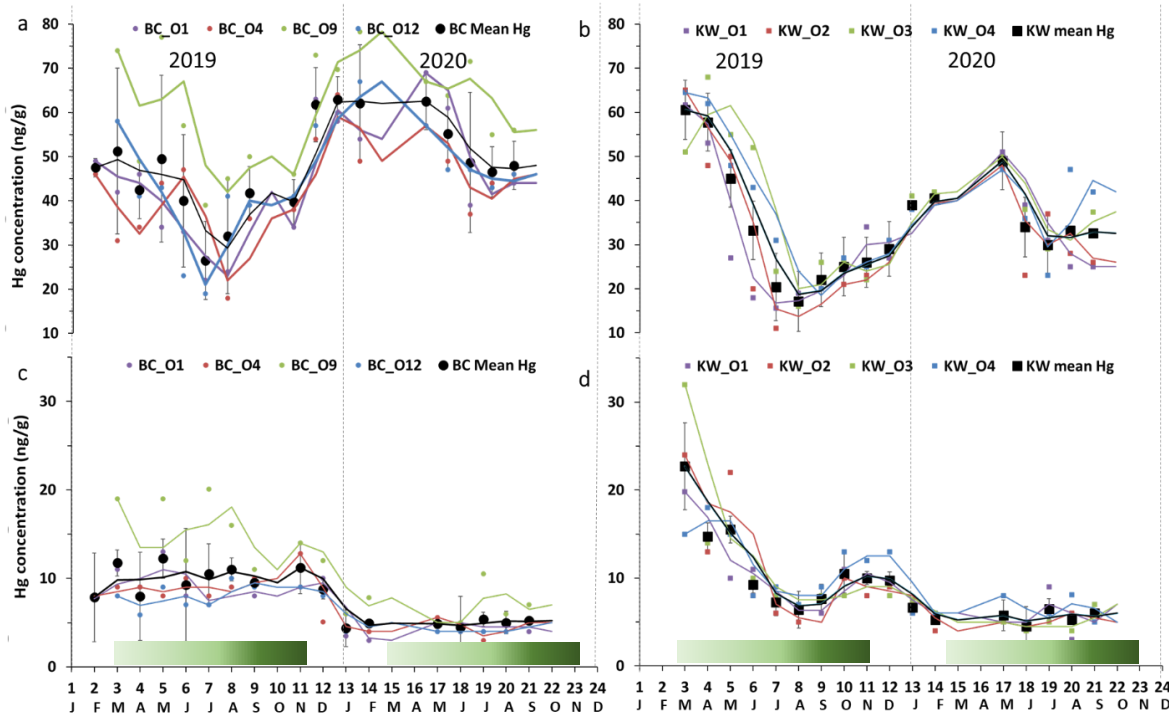
Figure 2. Seasonal variations of foliage Hg concentration in(**a**) Bchaaleh (BC) and (**b**) Kawkaba (KW) olive groves and stems Hg concentration in (**c**) Bchaaleh and (**d**) Kawkaba olive groves. Shaded green horizontal bars represent the leaf development of olive trees during the growing season of cultivars in Spain according to the BBCH scale (Sanz-Cortès et al., 2002).

3.3. Inter-individual variability between trees for each site

In the upper terrace of Bchaaleh grove, the foliage average Hg concentration of BCO4 and BCO1 varied between 42.4 ± 11.5 ng/g and 44.6 ± 13.3 ng/g respectively showing no significant difference (p-value = 0.8225). In the lower terrace of the same site, foliage average Hg concentrations of trees BCO12 and BCO9 were found to vary from 45.6 ± 12.7 ng/g to 60.7 ± 12.7 ng/g respectively (Figure 2a) exhibiting a significant difference ((p-value=0.0059). Tree BCO9 is significantly different to each of the three trees (p-value< 0.0059) while BCO1, BCO4 and BCO12 have very similar Hg contents (p-value= 0.46).

In the upper terrace of Bchaaleh grove, the stems average Hg concentration of BCO4 and BCO1 varied between 7.0 ± 2.8 ng/g and 7.1 ± 2.9 ng/g respectively showing no significant difference (p-value= 0.94). In the lower terrace, stems average Hg concentrations of BCO12 and BCO9 are 6.4 ± 2.2 ng/g and 11.2 ± 5.2 ng/g respectively showing a significant difference (p-value= 0.0054; Figure 2c). For BCO1 and BCO12 there was no significance difference (p-value= 0.5725), the same goes for BCO4 and BCO12 (p-value= 0.523).

The average concentration per tree in foliage and stems were 32.4 ± 12.2 ng/g and 8.5 ± 4.0 ng/g respectively for KWO1, 32. 8 ± 14.7 ng/g and 8.9 ± 6.0 ng/g for KWO2, 37.6 ± 14.0 ng/g and 9.3 ± 6.7 ng/g for KWO3 and 37.7 ± 13.6 ng/g and 9.6 ± 4.0 ng/g for KWO4 (Figure 2b,d). In Kawkaba grove, comparison of the foliage Hg concentration between the four studied trees shows no significant difference ($0.22 <$p-value< 1), neither for the stems ($0.21 <$p-value< 0.96).

3.4. Hg concentration and agro-climatic effect

At first glance, seasonal variations of the Hg concentrations of the foliage of both sites suggest a covariation with climatic parameters (Precipitation amounts, Relative Humidity and Temperature) (Figure SI) and atmospheric pCO_2. Foliage Hg content increased with higher precipitation and lower temperature (Autumn and Winter) while during the warmer and dryer seasons (May to mid-October), the Hg concentration of foliage decreased (Figure SI). However, the Wilcoxon test for a non-normal distribution shows no significant correlation between Hg concentration of foliage and precipitation (p-value= 0.95). While temperature, relative humidity and atmospheric CO_2 (pCO_2) shows a significant correlation (p-value = $2.2e^{-16}$). For the stems, Hg concentration also showed no significant correlation with precipitation (p-value= 0.1147), and a significant correlation with temperature, relative humidity and pCO_2 (p-value= $2.2e^{-16}$).

4. Discussion

4.1. Hg concentration in plant tissues, soil and litter in the studied groves

In both groves our values showed a higher Hg concentration in the olive foliage (Bchaaleh average of 48.1 ± 10.6 ng/g; Kawkaba average of 35.0 ± 12.4 ng/g), than that of the stems (Bchaaleh average of 7.9 ± 2.8 ng/g; Kawkaba average of 9.0 ± 4.7 ng/g) and that of olive fruits (7 ± 3.5 ng/g at Bchaaleh, n=3 and 11 ng/g in Kawkaba, n=1). Our

398 data corroborates previous studies (Bargagli 1995; Higueras et al. 2016) showing that olive foliage has the ~~main~~
399 highest Hg ~~content~~ concentration ~~among~~ of plant tissues. ~~Moreover, we demonstrate that~~ Our values are lower than
400 200 ng/g considered as Hg pollution threshold (Kabata-Pendias & Pendias, 2000) and ~~confirm~~ implying no pollution
401 effect for both Bchaaleh and Kawkaba groves (Table S2; Figure S3a,b). This ~~been said~~ suggests that our sites are good
402 remote bioindicators of the uptake of Hg through the plant, although more prolonged time range study is needed.
403 ~~Adding to that, the atmospheric Hg uptake in foliage dominates over Hg release (Pleijel et al., 2021). Since normally~~
404 ~~the main source of Hg into the foliage is atmospheric and minimally through the soil, this explains the higher Hg~~
405 ~~concentration in the foliage, while in the stems the main uptake is from the soil and it seems to be minimal (Tomiyasu~~
406 ~~et al., 2005) explaining the much lower level of Hg concentration in the stems than that in the foliage.~~ However, in
407 an overview of vegetation uptake of mercury and impacts on global cycling, Zhou et al., (2021) suggested lower values
408 for unpolluted sites (litterfall 43 ng/g > foliage 20 ng/g and branch 12 ng/g). Knowing that our sites correspond to
409 unpolluted areas of Lebanon, the lower values of Zhou et al., (2021) obtained from an ensemble of various species
410 (trees and grasses) and not specifically on olive trees, we considered that the threshold value of 200 ng/g (Kabata-
411 Pendias and Pendias 2000) is more adapted to our comparison.
412 As described in several studies, Hg in foliage originates predominantly from the atmospheric gaseous Hg(0) through
413 stomatal uptake (Ericksen et al., 2003; Lindberg et al., 1979; Zhou et al., 2021). Adding to that, the atmospheric Hg
414 uptake in foliage excedes Hg stomatal re-emission (Pleijel et al., 2021; Zhou et al., 2021). Inside the leaves the oxidized
415 Hg(II) has high affinities to bind covalently with organic groups (Du & Fang, 1983; Clarkson & Magos, 2006; Pleijel
416 et al., 2021). The Hg can be translocated by phloem transport to the stems and eventually into roots and potential
417 release into soils may also be contributing to Hg accumulation in soils (Giesler et al., 2017; Schaefer et al., 2020).
418 The soil surface and litter registered the highest Hg concentration (62 to 129 ng/g) among all samples (foliage, stems,
419 fruit) in both groves (Table 1) suggesting that the soil is the main Hg reservoir through the Hg throughfall and litter
420 inputs (Tomiyasu et al., 2005). Our findings are in agreement with studies on evergreen forest ecosystems reporting
421 that soil can hold more than 60 % of Hg input to the forest floor (Wang et al. 2016). Our soil surface sites values (61.9
422 $\pm$ 20.0 ng/g in Bchaaleh and 128.5 $\pm$ 9.4 ng/g in Kawkaba) show higher Hg concentration in Kawkaba compared to
423 the general background level of Hg as defined by uncontaminated soil world reference mean Hg contents (20 to 100
424 ng/g; Kabata-Pendias and Pendias 2000; Senesil et al. 1999; Gworek et al. 2020). However, both sites have
425 significantly lower values compared to known industrial and mining contaminated sites (> 1000 ng/g ;). Nevertheless,
426 studies conducted in different sites show a wide range of natural background Hg levels (ie. topsoils in Europe, India,
427 Brazil, Norwegian Arctic, New Zealand have values of 40, 50, 80, 110, 230 ng/g respectively) (Gworek et al. 2020)
428 making it difficult to set a specific Hg threshold value for uncontaminated soil (Table S2; Figure S3c). Due to the
429 differences registered in different countries and sites of sampled soil, this indicates a link with chemical and
430 mineralogical soil properties (ie. pH, humic acid, soil grain size distribution, organic matter type and clay percentage)
431 affecting Hg in soil and its transport (Richardson et al., 2013; Chen et al., 2016; O'Connor et al., 2019). Nitrogen can
432 also be a factor affecting the Hg content in soil depending on its characteristics. Nitrogen increase can change the
433 equilibrium of soil solution and the morphology of roots, causing a possible increase in Hg availability in soil and
434 increases the Hg uptake by the plant (Alloway, 1995; Barber, 1995; Carrasco-Gil et al., 2012). The increase in Hg

availability in the soil is due to the organic Nitrogen that provides a high absorption capacity, retaining the atmospheric Hg deposition (Obrist et al., 2009). Nitrogen supply prevents oxidative stress in roots, but also can improve root development and increase the uptake of Hg from the soil (Carrasco-Gil et al. 2012). Hence, we suggest that lower values in Bchaaleh soils are likely explained by the low clay, organic carbon and nitrogen contents (10.7 %, 4 % and 0.3 % in soil surface respectively).While Kawkaba higher Hg soil contents can be explained by the higher clay proportion (66 %) and organic carbon and nitrogen contents (9 % and 0.92 %). On such clay loam soils and rich organic matter, Hg binding is facilitated explaining higher content (O'Connor et al. 2019). ~~Moreover, the higher temperatures and lower precipitation and altitude in Kawkaba can be responsible for a higher dry deposition from gaseous elementary Hg in the forest floor (Teixeira et al. 2017).~~

~~In parallel,~~ The litter showed higher Hg concentration than that in foliage in both Bchaaleh (62.9 ± 17.8 ng/g) and Kawkaba (75.7 ± 20.3 ng/g) (Table 1). This has been also described by Rea et al., (1996) and Zhou et al., (2021) in uncontaminated and contaminated sites where litterfall Hg contents were systematically higher than the foliage Hg contents. The bacterial and chemical decomposition of the litter decrease significantly the amount of C compared to the Hg that conversely may continue to increase due to the continued absorption of Hg from precipitation and throughfall (Obrist et al., 2011; Pokharel & Obrist, 2011; Zhou et al., 2021). Another possible explanation is that the leaves shed as litter are likely to mostly be the oldest leaves which have accumulated Hg during the longest period of time and thus have higher Hg concentrations than the remaining foliage have on average since they consist of both younger and older foliage (Rea et al. 1996; Pleijel et al. 2021).

4.2. Seasonal foliage Hg content versus seasonal atmospheric Hg and CO$_2$

The late winter-early spring registered the highest Hg concentration for foliage in both groves, while summer and early fall to a less extent recorded the lowest concentrations. ~~Unexpectedly, we found a good positive covariation between Hg contents of our olive tree foliage and that of the atmosphere in the Northern Hemisphere (Jiskra et al. 2018). According to (Obrist, 2007), the observed maximum Hg$_{atm}$ (from October to March) can be explained by the anthropogenic and natural Hg emissions (ie. soil carbon mineralization, plant dormancy, net respiration of the global forest ecosystems) exceeding Hg burial processes (ie. Photosynthetic activity and stomatal conductance, forest floor Hg uptakes).~~ This seasonal change is explained by the seasonal tree physiology variations such as the Hg accumulation in leaves after stomatal uptake (Pleijel et al., 2021; Wohlgemuth et al., 2021). We can suggest that during winter-early spring, water is available and photosynthetic activity is not limited, hence both CO$_2$ and Hg diffuse through opened stomata inside the foliage. As shown on figure 2, Hg in foliage is low in summer-fall and hence act as a sink of Hg. Note that despite we mixed three generations of olive leaves (year N to N-3), the most recent of which are known to be low in mercury (Pleijel et al., 2021), the seasonal signal is still very remarkable. Therefore, one can speculate that the mercury levels would have been higher if we had avoided the recently formed foliage during spring and early summer. This may also explain the large difference in Hg levels between litter and foliage.

At our latitudes, Bchaaleh and Kawkaba foliage evergreen olive trees show a decrease in Hg contents from end of March to late August, with minimum values centered in August suggesting a decline of the plant Hg uptake likely explained by the reduction of the stomatal conductance (Lindberg et al., 2007; Pleijel et al., 2021). This minimal

photosynthetic activity occurs during the driest season (0 mm precipitation) and hottest temperatures (above 25°C) at our sites. Year 2020 has higher foliage Hg values than 2019. This can be related to a higher vegetation uptake in 2020 in comparison to 2019. Martino et al., (2022) showed seasonal variability of Gaseous Elemental Mercury (GEM) in the atmosphere in southern Italy (Figure 3a). They also related this seasonality to high energy use for heat during winter thus higher emissions due to coal combustion (Weigelt et al., 2015) and the effect of air mass trajectory on the GEM seasonality where the winter peak is connected to the Hg re-emission from sea surface and with long-range transport, in addition to the GEM oxidation rate in warmer months (Horowitz et al., 2017; Martino et al., 2022). Martino et al. (2022) comparing the normalized difference vegetation index values (NDVI) with GEM concentration of the same seasons over the different years (2018 to 2020), show that the higher vegetation uptake explains the GEM depletion in certain seasons and years. This was also collaborating Jiskra et al., (2018) for the Northern Hemisphere site. Since no data of atmospheric mercury in Lebanon or surrounding countries are available we used the atmospheric Hg time series data of Martino et al. (2022) (Figure 3a). We observed opposite trends between foliage Hg concentration and air Hg (negative covariation in 2019 and positve covariation in 2020) (Figure a,d,e).

Unexpectedly, We found a good positive covariation between Hg contents of our olive tree foliage and that of the atmosphere in the Northern Hemisphere (Jiskra et al. 2018). According to Obrist, (2007), the observed maximum Hg$_{atm}$ (from October to March) can be explained by the anthropogenic and natural Hg emissions (ie. soil carbon mineralization, plant dormancy, net respiration of the global forest ecosystems) exceeding Hg burial processes (ie. accumulation in foliage after stomatal uptake, forest floor Hg uptakes).This author discussed the significant role of the northern hemisphere vegetation and forest floor respiration and suggested that the decreasing atmospheric Hg content starting in March and reaching the minimal values in July August is likely attributable to the plant uptakes and precipitation (D. Obrist, 2007; Siudek et al., 2016; Jiskra et al., 2018). However at our latitudes, BC and KW foliage evergreen olive trees show also a decrease in Hg contents from end of March to late September, with minimum values centered in August suggesting a decline of the plant Hg uptake likely explained by the reduction of the stomatal conductance (Lindberg et al. 2007; Pleijel et al. 2021). This minimal photosynthetic activity occurs during the driest (0 mm precipitation) and hottest temperatures (above 25°C) at our sites. While the increase of the Hg intake starting in September and reaching its maximum in March occurs during the increasing Northern Hemisphere atmospheric Hg (Figure 3a,b). In different Olive cultivars from Italy, Proietti and Famiani (2002) show that lowest photosynthetic activity occur during summer (August) but also in winter (December) which is not supported by our data. The positive covariation between our olive foliage and atmospheric Hg contents do not support the hypothesis of Obrist 2007 and Jiskara et al. 2018 previous cited studies showing a strong depletion of atmospheric Hg concomitant to vegetation uptake in summer period uptakes (Obrist 2007; Jiskra et al. 2018). Two hypotheses can explain such positive correlations between our plant foliage and air Hg concentrations. Taking into account Hg results obtained during several seasonal campaigns in the surface waters of the Mediterranean Sea and the above atmospheric layer, it has been evidenced that the highest Hg fluxes to the atmosphere occur mainly in summer (Kotnik et al. 2014; Wangberg et al. 2001) and a higher total gaseous mercury (TGM) is registered in the eastern Mediterranean compared with the western Mediterranean and Northern Europe (Wängberg et al., 2001). Hence, we can hypothesis that a reverse Hg

509 ~~seasonal cycle in the Eastern Mediterranean would stand on a different seasonal atmospheric Hg variation than in the~~

510 ~~Northern Hemisphere~~.

511 Alternatively other studies reported a positive correlation between atmospheric Hg and crops (Niu et al. 2011) as

512 observed in our study between the $Hg_{foliage}$ and the atmospheric Hg in 2020 (Figure 3a,d,e). This suggest the hypothesis

513 where our groves seasonally exposed to high atmospheric Hg, accumulate Hg in their foliage (Lindberg et al. 2007;

514 Pleijel et al. 2021). According to Hanson et al. (1995), a compensation point for Hg uptake by plant foliage can be

515 considered but no information to our knowledge is available for the specific case of the olive trees. The tight link

516 between foliage Hg uptake and stomatal conductance seasonal variations can be also deduced from the analysis of the

517 partial pressure of the pCO_{2atm} seasonal variation (Obrist, 2007; Jiskra et al., 2018; Obrist et al., 2018; Pleijel et al.,

518 2021) (Figure 3b,d,e). Very good covariation between olive foliage Hg and pCO_{2atm} are shown for Bchaaleh and

519 Kawkaba despite a notable offset of one month at Kawkaba to two months at Bchaaleh can be deduced (Figure S4).

520 Taking into account our calculated time lags, we obtained significant correlations between our foliage Hg content and

521 pCO_{2atm} of 0.718 and 0.704 in Bchaaleh and Kawkaba respectively. Interestingly a one month time-lag between

522 atmospheric Hg and pCO_{2atm} is also reported by Jiskra et al. (2018) for most northern hemisphere sites. The offset of

523 one to two months between maxima of Bchaaleh and Kawkaba foliage Hg (March/April) and pCO_{2atm} (May) suggests

524 that the minimum of Hg in the foliage occur during the decreasing phase of the pCO_{2atm} when the global northern

525 hemisphere tend to become a net sink of CO_2. When minimum values of pCO_{2atm} are reached at the end of the dry

526 summer (Figure 3b), concomitant to minimum atmospheric Hg (Figure 3a), end of the drought and increase of

527 precipitation (Figure 3c), Bchaleh and Kawkaba olive trees show a recovery in the Hg uptake rates. The photosynthetic

528 activity and the stomatal conductance related to the climatic parameters (temperature, precipitation, humidity, pCO_2)

529 as shown by Ozturk et al. (2021) and the atmospheric Hg explain our foliage Hg seasonal cycle. At a regional scale,

530 our sites show different time lags between Bchaaleh and Kawkaba that we cannot explain fully except their altitudinal

531 differences, which can suggest that Bchaaleh grove benefits of less drought in summer. This can also be explained by

532 the physiology of olive trees that is characterised by small foliage surface area as a response to the high temperature

533 and less humidity in summer and the stomatal conductance in the foliage that increase in winter and decrease in

534 summer. As per Connor & Fereres, 2010, the olive tree is a day neutral plant were its reproductivity is affected by

535 temperature and sunlight. Its vegetative growth is limited by the low temperature in the winter season and water supply

536 in the summer season. The water loss from the foliage due to transpiration and temperature, creates a replacement for

537 water source to be the soil through the roots. The xylem being the main transporter between the roots and the canopy.

538 During the day the evaporation increase and the plant water content decreases and become minimal during midday,

539 noting that the soil water content is high. During the evening the olive tree seeks soil water as an equilibrium. If soil

540 water is not available enough to cover the olive need, the evergreen olive is able to adapt through conservation of

541 internal water especially during severe summer drought, due to its ability to restrict water loss to the atmosphere and

542 maximize extraction of soil water (Connor & Fereres, 2010). Taking into account Hg results obtained during several

543 seasonal campaigns in the surface waters of the Mediterranean Sea and the above atmospheric layer, it has been

544 evidenced that the highest Hg fluxes to the atmosphere occur mainly in summer (Wangberg et al. 2001; Kotnik et al.

545 2014). Moreover, a higher total gaseous mercury (TGM) is registered in the eastern Mediterranean compared with the

546 western Mediterranean and Northern Europe (Wängberg et al., 2001). Olive trees are known to be a mycotrophic
547 plant. Mycorrhiza acts as a barrier that restrict the movement of heavy metals from the roots to the plants (Wu et al.,
548 2016; Riaz et al., 2021). In the Mediterranean region, it is reported that intensity of mycorrhizal colonization of olive
549 tree roots increases with the increase of seasonal precipitation/decrease in temperature and decreased with the increase
550 of air temperature, when it is drier (Meddad-Hamza et al., 2017). This confirms that in the decrease of mycorrhizal
551 activity in summer, a possible minimal Hg uptake from the soil and roots to the foliage and stems through water during
552 the drought season may occur (Rea et al., 2002; Meddad-Hamza et al., 2017). Further analysis and data are necessary
553 to confirm the above assumption.
554
555
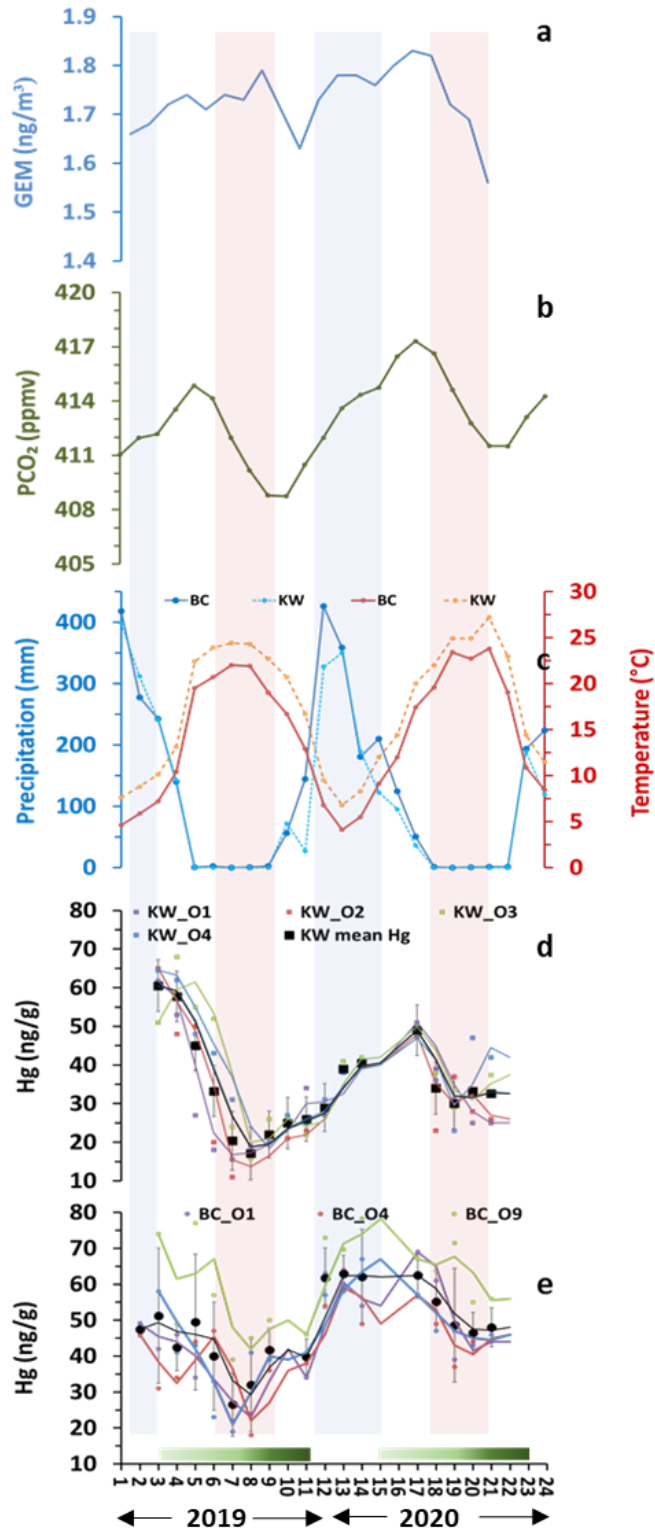
556
557 **Figure 3**. Seasonal variations of (**a**) atmospheric Hg(0) (Martino et al. 2022), (**b**) pCO₂ (NOAA Global Monitoring
558 Laboratory), (**c**) precipitations and temperature of Bchaaleh and Kawkaba respectively and (**d**) and (**e**) foliage Hg
559 concentration in Bchaaleh and Kawkaba olive groves respectively. Shaded green horizontal bars represent the leaf
560 development of olive trees during the growing season of cultivars in Spain according to the BBCH scale (Sanz-Cortès
561 et al., 2002). Shaded colored lines correspond to the Winter (Blue) and Summer (Red).

4.3. Hg cycling in the stems, litter and soil system

For each site, Hg contents in stems exhibit narrow range between the different trees except tree BCO9, which had the highest stem values. We speculate that this higher Hg content is the adjunction of chemical products as fertilizer on the plot 549 belonging to a different owner (Figure S2) likely between fall and winter. It was observed by (Zhao & Wang, 2010) that the fertilizer used and its source of phosphorous may affect the Hg content in the product and thus affect the amount of Hg transported into the fertilized soil.

At a seasonal scale, the averaged Hg values of soil system show statistical significance differences between the four seasons, while stems show a significant difference between winter (lowest values) and spring (p-value= 0.030) and winter-autumn (p-value= 0.047) in Bchaaleh grove mostly similar to foliage changes. While litter shows no significant difference between seasons. The same behavior was registered in Kawkaba in litter and soils, while stems showing statistical significance differences between autumn and spring (p-value= 0.011), spring-winter (p-value= 0.006) and spring-summer (p-value= 0.004) (Table 2). Despite the small amount of Hg content in the stems, the statistically significant seasonal changes may suggest that small amount of Hg move from the foliage to the lignified tissues as stems. However, we cannot neglect the Hg transport in xylem sap from the roots to the aboveground plant tissues even if minimal (Yang et al. 2018).

We can suggest the following Hg cycling in the system of the olive grove/soil. In winter-early spring the highest concentrations in foliage continuously feed the litter and can explain the following maximal spring Hg content of the litter. The decomposition of the litter organic matter during the wettest conditions likely liberate Hg in the Hg(0) or Hg(II) forms or MeHg either towards the atmosphere or the surface soil (see Table 2) respectively (Gworek et al., 2020). A fraction of the degraded organic matter is transferred through gaseous evaporative processes towards the atmosphere while another fraction of the Hg is leaching towards the deeper soil in addition to dry Hg deposition during dry season (Teixeira et al. 2017). We can also speculate that the small Hg decrease observed in soil 0-30, 30-60 cm during the winter season in Bchaaleh can be due to the minimal absorption of total Hg and MeHg through the roots and xylem sap to the above ground tissues (Johnson and Lindberg 1995).

4.3.2. Hg uptake in foliage: atmospheric or soil sources?

In sites without local contamination, as those presented in this study, no significant correlation between the foliage and soil Hg content is observed, in agreement with Higueras et al. (2012). In contaminated sites, a strong correlation between foliage and soil Hg content has been reported (Higueras et al. 2016). Interestingly, in the Mediterranean region, it is reported that intensity of mycorrhizal colonization of olive tree roots increases with the increase of seasonal precipitation/decrease in temperature and decreased with the increase of air temperature, when it is drier (Meddad Hamza et al. 2017). This is an independent argument to support the atmosphere being the main Hg source to the foliage during the wet seasons, but also confirming in absence of mycorrhizal activity a possible minimal Hg uptake from the soil to the foliage and stems through water during the drought season (Rea et al. 2002; Meddad Hamza et al. 2017). Eventually, we suggest that the main source of Hg for both olive groves is the atmospheric mercury.

5. Conclusion

This is the first study conducted on monumental olive trees in a ~~non-contaminated~~ remote site of the MENA region without local contamination and followed at a monthly basis over 18 months. Findings of our study ~~in remote sites without local contamination~~ indicate a higher uptake of Hg in the olive foliage compared to stems, fruits items and a remarkable $Hg_{Foliage}$ seasonal variation in both studied groves. Winter and Spring were particularly suitable for Hg accumulation in foliage in both sites. The significant correlation between our $Hg_{Foliage}$ contents and the atmospheric Hg content and pCO_2, despite the one to two months' time lag, suggests that the main source of $Hg_{Foliage}$ is the atmospheric Hg as observed in different species and studies (conifers and hardwood). Hg is absorbed by the foliage, via the open stomata, driven by the interaction of high vegetal activity, temperature, water availability and the processes that control transpiration, which is likely to be seasonal. Hence physiological and climatic processes explain the seasonal Hg accumulation in foliage. Thus, a more intensive study taking account the phenological dynamics of olive tree foliage must be focused on. ~~and more intensive studies on soil and litter is needed to be able to assess the source of Hg uptake in the olive trees.~~ Further comparison and studies on the seasonal atmospheric Hg in the eastern Mediterranean basin are necessary to test our hypothesis of the reversed seasonality of Hg in 2019 and positive covariation in 2020 since contrary to the global Northern Hemisphere and western Mediteranean region vegetation, our olive groves act as a sink of Hg and CO_2 when global Northern and western Mediterranean vegetation is emitting. This relationship $Hg_{Foliage} - Hg_{atm}-pCO_{2atm}$ should be further investigated along the season and locally to better understand the observed time lags. Soil surface registered the highest Hg concentration among all studied compartments due to well-known processes of litter and throughfall that incorporate Hg to the soil surface. Moreover, this study highlights significant differences between Hg_{soil} in Bchaaleh and Kawkaba groves due to differences in soil characteristics. In this study we worked on the present time samples in order to have a better understanding of the Hg cycle in the olive tree. ~~A second step would be to reconstruct the paleo-evolution through also studying tree rings Hg concentration were we can also identify a seasonal variation.~~ Our main contribution in this study is to see how the present-day olive trees records some elements such as Hg to better understand how the Hg in tree rings could be used for the past accumulation records.

Data availability

The datasets generated during and/or analyzed during the current study are available from the corresponding author on reasonable request.

Author Contributions
The corresponding author **Ilham Bentaleb** is responsible for ensuring that the descriptions are accurate and agreed upon by all authors. Conceptualization and methodology were done and developed by **Ilham Bentaleb** and **Lamis Chalak**. The material collection was performed by **Nagham Tabaja**, **Ilham Bentaleb**, **Lamis Chalak**, **Ihab Jomaa, and Milad Riachy**. Sample storage and preparation in Lebanon organized by **Nagham Tabaja**. Material preparation at ISEM by **Nagham Tabaja**, Data collection and analysis were performed by Nagham Tabaja, **Ilham Bentaleb**, **David Amouroux, and Emmanuel Tessier**. The setting of the meteorological stations by **Ihab Jomaa**. Subsamples of soil were analyzed for carbon and nitrogen elemental contents (%) by **François Fourel**. The first draft of the manuscript was written **by Nagham Tabaja**. **Ilham Bentaleb, Lamis Chalak**, **David Amouroux, Ihab Jomaa, and Milad Riachy** commented

640 on previous versions of the manuscript. All authors read and approved the final manuscript. Supervision was done by
641 Ilham Bentaleb and Lamis Chalak.
642
643

644 **Competing interests**
645 The authors declare that they have no known competing financial interests or personal relationships that could have
646 appeared to influence the work reported in this paper.
647
648
649 **Acknowledgments**

650 The authors would like to acknowledge the National Council for Scientific Research of Lebanon (CNRS-L) and
651 Montpellier University for granting a doctoral fellowship (CNRS-L/UM) to Nagham Tabaja. The authors would also
652 like to thank the Franco-Lebanese Hubert Curien Partnership (PHC-CEDRE) project 44559PL for the funding
653 provided. Institute of Evolutionary Science of Montpellier (ISEM) at Montpellier University and the Research
654 Platform for Environment and Science- Doctoral School of Science and Technology (PRASE-EDST) at the Lebanese
655 University are also acknowledged for their support of the laboratory work. Credits go to the Lebanese Agriculture
656 Research Institute (LARI) for assuring automated weather stations and manual rain gauges per site. The authors are
657 grateful to the Municipality of Bchaaleh (Mr. Rachid Geagea) and the Municipality of Kawkaba (Ms. Mira Khoury).
658 Acknowledgments are extended to Ms. Amira Yousef at LARI for her kind support and to Mr. Akram Tabaja for
659 helping during fieldwork. We are very greatful to Pleijel Hakan who reviewed this article improving significantly our
660 paper. We deeply aknowledgeAndrew Johnston for the English revision.
661
662

663 **Funding**
664 This work was supported and funded by Lebanon and Montpellier University (CNRS-L/UM grant), and PHC-
665 CEDRE-project 44559PL

666

667 **References**
668
669 **References**
670

671 Abou Habib, N., Taleb, M., & Khoury, R. (2015). *Environmental and social safeguard studies*

672 *for lake qaraoun pollution prevention project*. *V1*(E4749).

673 Alcaras, L. M. A., Rousseaux, M. C., & Searles, P. S. (2016). Responses of several soil and plant

674 indicators to post-harvest regulated deficit irrigation in olive trees and their potential for

675 irrigation scheduling. *Agricultural Water Management*, *171*, 10–20.

676 https://doi.org/10.1016/j.agwat.2016.03.006

677 Alloway, B. J. (1995). *Heavy Metals in Soils*. Springer Science & Business Media.

678 Al-Zubaidi, A., Yanni, S., & Bashour, I. (2008). Potassium status in some Lebanese soils.

679 *Lebanese Science Journal*, *9*(1), 81–97.

680 Assad, M. (2017). *Transfert des éléments traces métalliques vers les végétaux: Mécanismes et*

681 *évaluations des risques dans des environnements exposés à des activités anthropiques.*

682 218.

683 Baayoun, A., Itani, W., El Helou, J., Halabi, L., Medlej, S., El Malki, M., Moukhadder, A.,

684 Aboujaoude, L. K., Kabakian, V., Mounajed, H., Mokalled, T., Shihadeh, A., Lakkis, I.,

685 & Saliba, N. A. (2019). Emission inventory of key sources of air pollution in Lebanon.

686 *Atmospheric Environment*, *215*, 116871. https://doi.org/10.1016/j.atmosenv.2019.116871

687 Badr, R., Holail, H., & Olama, Z. (2014). *Water quality assessment of hasbani river in south*

688 *lebanon: microbiological and chemical characteristics and their impact on the*

689 *ecosystem. 3*, 16.

690 Barber, S. A. (1995). *Soil Nutrient Bioavailability: A Mechanistic Approach*. John Wiley &

691 Sons.

692 Bargagli, R. (1995). The elemental composition of vegetation and the possible incidence of soil

693 contamination of samples. *Science of The Total Environment*, *176*(1–3), 121–128.

694 https://doi.org/10.1016/0048-9697(95)04838-3

695 Barre, J. P. G., Deletraz, G., Sola-Larrañaga, C., Santamaria, J. M., Bérail, S., Donard, O. F. X.,

696 & Amouroux, D. (2018). Multi-element isotopic signature (C, N, Pb, Hg) in epiphytic

697 lichens to discriminate atmospheric contamination as a function of land-use

698 characteristics (Pyrénées-Atlantiques, SW France). *Environmental Pollution*, *243*, 961–

699 971. https://doi.org/10.1016/j.envpol.2018.09.003

700 Beauford, W., Barber, J., & Barringer, A. R. (1977). Uptake and Distribution of Mercury within

701 Higher Plants. *Physiologia Plantarum*, *39*(4), 261–265. https://doi.org/10.1111/j.1399-

702 3054.1977.tb01880.x

703   Besnard, G., Khadari, B., Navascues, M., Fernandez-Mazuecos, M., Bakkali, A. E., Arrigo, N.,

704   Baali-Cherif, D., de Caraffa, V. B.-B., Santoni, S., Vargas, P., & Savolainen, V. (2013).

705   The complex history of the olive tree: From Late Quaternary diversification of

706   Mediterranean lineages to primary domestication in the northern Levant. *Proceedings of*

707   *the Royal Society B: Biological Sciences*, *280*(1756), 20122833–20122833.

708   Bishop, K. H., Lee, Y.-H., Munthe, J., & Dambrine, E. (1998). Xylem sap as a pathway for total

709   mercury and methylmercury transport from soils to tree canopy in the boreal forest.

710   *Biogeochemistry*, *40*, 101–113.

711   Bishop, K., Shanley, J. B., Riscassi, A., de Wit, H. A., Eklöf, K., Meng, B., Mitchell, C.,

712   Osterwalder, S., Schuster, P. F., Webster, J., & Zhu, W. (2020). Recent advances in

713   understanding and measurement of mercury in the environment: Terrestrial Hg cycling.

714   *Science of The Total Environment*, *721*, 137647.

715   https://doi.org/10.1016/j.scitotenv.2020.137647

716   Blackwell, B. D., & Driscoll, C. T. (2015). Using foliar and forest floor mercury concentrations

717   to assess spatial patterns of mercury deposition. *Environmental Pollution*, *202*, 126–134.

718   https://doi.org/10.1016/j.envpol.2015.02.036

719   Boening, D. W. (2000). *Ecological e€ ects, transport, and fate of mercury: A general review*. 17.

720   Borjac, J., El Joumaa, M., Kawach, R., Youssef, L., & Blake, D. A. (2019). Heavy metals and

721   organic compounds contamination in leachates collected from Deir Kanoun Ras El Ain

722   dump and its adjacent canal in South Lebanon. *Heliyon*, *5*(8), e02212.

723   https://doi.org/10.1016/j.heliyon.2019.e02212

724   Borjac, J., El Joumaa, M., Youssef, L., Kawach, R., & Blake, D. A. (2020). Quantitative

725   Analysis of Heavy Metals and Organic Compounds in Soil from Deir Kanoun Ras El Ain

726   Dump, Lebanon. *The Scientific World Journal*, *2020*, 1–10.

727   https://doi.org/10.1155/2020/8151676

728   Briffa, J., Sinagra, E., & Blundell, R. (2020). Heavy metal pollution in the environment and their

729   toxicological effects on humans. *Heliyon*, *6*(9), e04691.

730   https://doi.org/10.1016/j.heliyon.2020.e04691

731   Carrasco-Gil, S., Estebaranz-Yuberob, M., Medel-Cuestab, D., Millán, R., & Hernández, L. E.

732   (2012). Influence of nitrate fertilization on Hg uptake and oxidative stress parameters in

733   alfalfa plants cultivated in a Hg-polluted soil. *Environmental and Experimental Botany*,

734   *75*. https://doi.org/10.1016/j.envexpbot.2011.08.013

735   Cavallini, A., Natali, L., Durante, M., & Maserti, B. (1999). Mercury uptake, distribution and

736   DNA affinity in durum wheat (Triticum durum Desf.) plants. *Science of The Total*

737   *Environment*, *243–244*, 119–127. https://doi.org/10.1016/S0048-9697(99)00367-8

738   Chen, X., Ji, H., Yang, W., Zhu, B., & Ding, H. (2016). Speciation and distribution of mercury in

739   soils around gold mines located upstream of Miyun Reservoir, Beijing, China. *Journal of*

740   *Geochemical Exploration*, *163*, 1–9. https://doi.org/10.1016/j.gexplo.2016.01.015

741   Clarkson, T. W., & Magos, L. (2006). The Toxicology of Mercury and Its Chemical Compounds.

742   *Critical Reviews in Toxicology*, *36*(8), 609–662.

743   https://doi.org/10.1080/10408440600845619

744   Connor, D. J., & Fereres, E. (2010). The Physiology of Adaptation and Yield Expression in

745   Olive. In J. Janick (Ed.), *Horticultural Reviews* (pp. 155–229). John Wiley & Sons, Inc.

746   https://doi.org/10.1002/9780470650882.ch4

747   Dastoor, A., Angot, H., Bieser, J., Christensen, J. H., Douglas, T. A., Heimbürger-Boavida, L.-

748   E., Jiskra, M., Mason, R. P., McLagan, D. S., Obrist, D., Outridge, P. M., Petrova, M. V.,

749   Ryjkov, A., St. Pierre, K. A., Schartup, A. T., Soerensen, A. L., Toyota, K., Travnikov,

750   O., Wilson, S. J., & Zdanowicz, C. (2022). Arctic mercury cycling. *Nature Reviews Earth*

751   *& Environment*, *3*(4), Article 4. https://doi.org/10.1038/s43017-022-00269-w

752 Demers, J. D., Blum, J. D., & Zak, D. R. (2013). Mercury isotopes in a forested ecosystem:

753   Implications for air-surface exchange dynamics and the global mercury cycle: Mercury

754   isotopes in a forested ecosystem. *Global Biogeochemical Cycles*, *27*(1), 222–238.

755   https://doi.org/10.1002/gbc.20021

756 Du, S.-H., & Fang, S. C. (1983). Catalase activity of C3 and C4 species and its relationship to

757   mercury vapor uptake. *Environmental and Experimental Botany*, *23*(4), 347–353.

758   https://doi.org/10.1016/0098-8472(83)90009-6

759 Duval, B., Gredilla, A., Fdez-Ortiz de Vallejuelo, S., Tessier, E., Amouroux, D., & de Diego, A.

760   (2020). A simple determination of trace mercury concentrations in natural waters using

761   dispersive Micro-Solid phase extraction preconcentration based on functionalized

762   graphene nanosheets. *Microchemical Journal*, *154*, 104549.

763   https://doi.org/10.1016/j.microc.2019.104549

764 EJOLT. (2019). *Cimenterie Nationale Factory in Chekaa, Lebanon | EJAtlas*. Environmental

765   Justice Atlas. https://ejatlas.org/conflict/chekaa

766 Ericksen, J. A., Gustin, M. S., Schorran, D. E., Johnson, D. W., Lindberg, S. E., & Coleman, J.

767   S. (2003). Accumulation of atmospheric mercury in forest foliage. *Atmospheric*

768   *Environment*, *37*(12), 1613–1622. https://doi.org/10.1016/S1352-2310(03)00008-6

769 Ermolin, M. S., Fedotov, P. S., Malik, N. A., & Karandashev, V. K. (2018). Nanoparticles of

770   volcanic ash as a carrier for toxic elements on the global scale. *Chemosphere*, *200*, 16–

771   22. https://doi.org/10.1016/j.chemosphere.2018.02.089

772 Freeman, M., & Carlson, R. M. (2005). Essential nutrients. *Olive Production Manual*, *3353*, 75.

773 Friedli, H. R., Arellano, A. F., Cinnirella, S., & Pirrone, N. (2009). Initial Estimates of Mercury

774   Emissions to the Atmosphere from Global Biomass Burning. *Environmental Science &*

775   *Technology*, *43*(10), 3507–3513. https://doi.org/10.1021/es802703g

776 Galatali, S., A., N., & Kaya, E. (2021). *Characterization of Olive (Olea Europaea L.) Genetic*

777   *Resources via PCR-Based Molecular Marker Systems*. *2*, 26–33.

778   https://doi.org/10.24018/ejbio.2021.2.1.146

779 Gårdfeldt, K., Sommar, J., Ferrara, R., Ceccarini, C., Lanzillotta, E., Munthe, J., Wängberg, I.,

780   Lindqvist, O., Pirrone, N., Sprovieri, F., Pesenti, E., & Strömberg, D. (2003). Evasion of

781   mercury from coastal and open waters of the Atlantic Ocean and the Mediterranean Sea.

782   *Atmospheric Environment*, *37*, 73–84. https://doi.org/10.1016/S1352-2310(03)00238-3

783 Gérard, J., & Nehmé, C. (2020). Lebanon. *Méditerranée. Revue Géographique Des Pays*

784   *Méditerranéens / Journal of Mediterranean Geography*, *131*, Article 131.

785   https://journals.openedition.org/mediterranee/11018#

786 Giesler, R., Clemmensen, K. E., Wardle, D. A., Klaminder, J., & Bindler, R. (2017). Boreal

787   Forests Sequester Large Amounts of Mercury over Millennial Time Scales in the

788   Absence of Wildfire. *Environmental Science & Technology*, *51*(5), 2621–2627.

789   https://doi.org/10.1021/acs.est.6b06369

790 Grigal, D. (2003). Mercury Sequestration in Forests and Peatlands: A Review. *Journal of*

791   *Environmental Quality - J ENVIRON QUAL*, *32*. https://doi.org/10.2134/jeq2003.0393

792 Guarino, F., Improta, G., Triassi, M., Castiglione, S., & Cicatelli, A. (2021). Air quality

793   biomonitoring through Olea europaea L.: The study case of "Land of pyres."

794   *Chemosphere*, *282*, 131052. https://doi.org/10.1016/j.chemosphere.2021.131052

795   Gworek, B., Dmuchowski, W., & Baczewska-Dąbrowska, A. H. (2020). Mercury in the

796   terrestrial environment: A review. *Environmental Sciences Europe*, *32*(1), 128.

797   https://doi.org/10.1186/s12302-020-00401-x

798   Hanson, P. J., Lindberg, S. E., Tabberer, T. A., Owens, J. G., & Kim, K.-H. (1995). Foliar

799   exchange of mercury vapor: Evidence for a compensation point. *Water, Air, & Soil*

800   *Pollution*, *80*(1–4), 373–382. https://doi.org/10.1007/BF01189687

801   Higueras, P., Amorós, J. A., Esbrí, J. M., García-Navarro, F. J., Pérez de los Reyes, C., &

802   Moreno, G. (2012). Time and space variations in mercury and other trace element

803   contents in olive tree leaves from the Almadén Hg-mining district. *Journal of*

804   *Geochemical Exploration*, *123*, 143–151. https://doi.org/10.1016/j.gexplo.2012.04.012

805   Higueras, P. L., Amorós, J. Á., Esbrí, J. M., Pérez-de-los-Reyes, C., López-Berdonces, M. A., &

806   García-Navarro, F. J. (2016). Mercury transfer from soil to olive trees. A comparison of

807   three different contaminated sites. *Environmental Science and Pollution Research*, *23*(7),

808   6055–6061. https://doi.org/10.1007/s11356-015-4357-2

809   Horowitz, H. M., Jacob, D. J., Zhang, Y., Dibble, T. S., Slemr, F., Amos, H. M., Schmidt, J. A.,

810   Corbitt, E. S., Marais, E. A., & Sunderland, E. M. (2017). A new mechanism for

811   atmospheric mercury redox chemistry: Implications for the global mercury budget.

812   *Atmospheric Chemistry and Physics*, *17*(10), 6353–6371. https://doi.org/10.5194/acp-17-

813   6353-2017

814   Jindrich Petrlik, Kodeih, N., IndyACT, Arnika Association, & IPEN WG. (2013). *Mercury in*

815   *Fish and Hair Samples from Batroun, Lebanon*.

816   https://doi.org/10.13140/RG.2.2.12052.40327

817   Jiskra, M., Sonke, J. E., Obrist, D., Bieser, J., Ebinghaus, R., Myhre, C. L., Pfaffhuber, K. A.,

818   Wängberg, I., Kyllönen, K., Worthy, D., Martin, L. G., Labuschagne, C., Mkololo, T.,

819   Ramonet, M., Magand, O., & Dommergue, A. (2018). A vegetation control on seasonal

820   variations in global atmospheric mercury concentrations. *Nature Geoscience*, *11*(4), 244–

821   250. https://doi.org/10.1038/s41561-018-0078-8

822   Johnson, & Lindberg. (1995). The biogeochemical cycling of Hg in forests: Alternative methods

823   for quantifying total deposition and soil emission. *1995*, *80: 1069–1077*, 9.

824   Jurdi, M., Korfali, S. I., Karahagopian, Y., & Davies, B. E. (2002). *Evaluation of Water Quality*

825   *of the Qaraaoun Reservoir, Lebanon: Suitability for Multipurpose Usage*. *77*(11–30), 20.

826   Kabata-Pendias, A., & Pendias, H. (2000). *Trace elements in soils and plants* (3rd ed). CRC

827   Press.

828   Khadari, B., El Bakkali, A., Essalouh, L., Tollon, C., Pinatel, C., & Besnard, G. (2019).

829   Cultivated Olive Diversification at Local and Regional Scales: Evidence From the

830   Genetic Characterization of French Genetic Resources. *Frontiers in Plant Science*, *10*.

831   https://www.frontiersin.org/articles/10.3389/fpls.2019.01593

832   Kobrossi, R., Nuwayhid, I., Sibai, A. M., El-Fadel, M., & Khogali, M. (2002). Respiratory health

833   effects of industrial air pollution on children in North Lebanon. *International Journal of*

834   *Environmental Health Research*, *12*(3), 205–220.

835   https://doi.org/10.1080/09603/202/000000970

836   Kotnik, J., Sprovieri, F., Ogrinc, N., Horvat, M., & Pirrone, N. (2014). Mercury in the

837   Mediterranean, part I: Spatial and temporal trends. *Environmental Science and Pollution*

838   *Research*, *21*(6), 4063–4080. https://doi.org/10.1007/s11356-013-2378-2

839   Labdaoui, D., Lotmani, B., & Aguedal, H. (2021). Assessment of Metal Pollution on the

840   Cultivation of Olive Trees in the Petrochemical Industrial Zone of Arzew (Algeria).

841   *South Asian Journal of Experimental Biology*, *11*(3), Article 3.

842   https://doi.org/10.38150/sajeb.11(3).p227-233

843   *Lebanon: Air Pollution | IAMAT*. (2020). https://www.iamat.org/country/lebanon/risk/air-

844   pollution

845   Li, D., Fang, K., Li, Y., Chen, D., Liu, X., Dong, Z., Zhou, F., Guo, G., Shi, F., Xu, C., & Li, Y.

846   (2017). Climate, intrinsic water-use efficiency and tree growth over the past 150 years in

847   humid subtropical China. *PLOS ONE*, *12*(2), e0172045.

848   https://doi.org/10.1371/journal.pone.0172045

849   Li, R., Wu, H., Ding, J., Fu, W., Gan, L., & Li, Y. (2017). Mercury pollution in vegetables,

850   grains and soils from areas surrounding coal-fired power plants. *Scientific Reports*, *7*(1),

851   46545. https://doi.org/10.1038/srep46545

852   Lindberg, S., Bullock, R., Ebinghaus, R., Engstrom, D., Feng, X., Fitzgerald, W., Pirrone, N.,

853   Prestbo, E., & Seigneur, C. (2007). A Synthesis of Progress and Uncertainties in

854   Attributing the Sources of Mercury in Deposition. *Ambio*, *36*(1), 19–32.

855   Lindberg, S. E., Jackson, D. R., Huckabee, J. W., Janzen, S. A., Levin, M. J., & Lund, J. R.

856   (1979). Atmospheric Emission and Plant Uptake of Mercury from Agricultural Soils near

857   the Almadén Mercury Mine. *Journal of Environmental Quality*, *8*(4), 572–578.

858   https://doi.org/10.2134/jeq1979.00472425000800040026x

859   Lodenius, M., Tulisalo, E., & Soltanpour-Gargari, A. (2003). Exchange of mercury between

860   atmosphere and vegetation under contaminated conditions. *Science of The Total*

861   *Environment*, *304*(1–3), 169–174. https://doi.org/10.1016/S0048-9697(02)00566-1

862   Luo, Y., Duan, L., Driscoll, C. T., Xu, G., Shao, M., Taylor, M., Wang, S., & Hao, J. (2016).

863   Foliage/atmosphere exchange of mercury in a subtropical coniferous forest in south

864   China. *Journal of Geophysical Research: Biogeosciences*, *121*(7), 2006–2016.

865   https://doi.org/10.1002/2016JG003388

866   Maillard, F., Girardclos, O., Assad, M., Zappelini, C., Pérez Mena, J. M., Yung, L., Guyeux, C.,

867   Chrétien, S., Bigham, G., Cosio, C., & Chalot, M. (2016). Dendrochemical assessment of

868   mercury releases from a pond and dredged-sediment landfill impacted by a chlor-alkali

869   plant. *Environmental Research*, *148*, 122–126.

870   https://doi.org/10.1016/j.envres.2016.03.034

871   Martino, M., Tassone, A., Angiuli, L., Naccarato, A., Dambruoso, P. R., Mazzone, F., Trizio, L.,

872   Leonardi, C., Petracchini, F., Sprovieri, F., Pirrone, N., D'Amore, F., & Bencardino, M.

873   (2022). First atmospheric mercury measurements at a coastal site in the Apulia region:

874   Seasonal variability and source analysis. *Environmental Science and Pollution Research*,

875   *29*(45), 68460–68475. https://doi.org/10.1007/s11356-022-20505-6

876   McLagan, D. S., Biester, H., Navrátil, T., Kraemer, S. M., & Schwab, L. (2022). *Internal tree*

877   *cycling and atmospheric archiving of mercury: Examination with concentration and*

878   *stable isotope analyses* [Preprint]. Biogeochemistry: Air - Land Exchange.

879   https://doi.org/10.5194/bg-2022-124

880   McLagan, D. S., Stupple, G. W., Darlington, A., Hayden, K., Steffen, A., & Kamp, L. (2021).

881   Where there is smoke there is mercury: Assessing boreal forest fire mercury emissions

882   using aircraft and highlighting uncertainties associated with upscaling emissions

883   estimates. *Atmos. Chem. Phys.*, 19.

884   Meddad-Hamza, A., Hamza, N., Neffar, S., Beddiar, A., Gianinazzi, S., & Chenchouni, H.

885   (2017). Spatiotemporal variation of arbuscular mycorrhizal fungal colonization in olive (

886   Olea europaea L.) roots across a broad mesic-xeric climatic gradient in North Africa.

887   *Science of The Total Environment*, *583*, 176–189.

888   https://doi.org/10.1016/j.scitotenv.2017.01.049

889   Naharro, R., Esbri, J., Amorós, J., & Higueras, P. (2018). *Atmospheric mercury uptake and*

890   *desorption from olive-tree leaves*. *20*(EGU2018-2982,2018), 2.

891   Nassif, N., Jaoude, L. A., El Hage, M., & Robinson, C. A. (2016). Data Exploration and

892   Reconnaissance to Identify Ocean Phenomena: A Guide for InSitu Data Collection.

893   *Journal of Water Resource and Protection*, *08*(10), 929–943.

894   https://doi.org/10.4236/jwarp.2016.810076

895   Niu, Z., Zhang, X., Wang, Z., & Ci, Z. (2011). Field controlled experiments of mercury

896   accumulation in crops from air and soil. *Environmental Pollution*, *159*(10), 2684–2689.

897   https://doi.org/10.1016/j.envpol.2011.05.029

898   Obrist, D. (2007). Atmospheric mercury pollution due to losses of terrestrial carbon pools?

899   *Biogeochemistry*, *85*(2), 119–123. https://doi.org/10.1007/s10533-007-9108-0

900   Obrist, D., Johnson, D. W., & Lindberg, S. E. (2009). *Mercury concentrations and pools in four*

901   *Sierra Nevada forest sites, and relationships to organic carbon and nitrogen*. 13.

902   Obrist, D., Kirk, J. L., Zhang, L., Sunderland, E. M., Jiskra, M., & Selin, N. E. (2018). A review

903   of global environmental mercury processes in response to human and natural

904   perturbations: Changes of emissions, climate, and land use. *Ambio*, *47*(2), 116–140.

905   https://doi.org/10.1007/s13280-017-1004-9

906 Obrist, M. K., Rathey, E., Bontadina, F., Martinoli, A., Conedera, M., Christe, P., & Moretti, M.

907   (2011). Response of bat species to sylvo-pastoral abandonment. *Forest Ecology and*

908   *Management*, *261*(3), 789–798. https://doi.org/10.1016/j.foreco.2010.12.010

909 O'Connor, D., Hou, D., Ok, Y. S., Mulder, J., Duan, L., Wu, Q., Wang, S., Tack, F. M. G., &

910   Rinklebe, J. (2019). Mercury speciation, transformation, and transportation in soils,

911   atmospheric flux, and implications for risk management: A critical review. *Environment*

912   *International*, *126*, 747–761. https://doi.org/10.1016/j.envint.2019.03.019

913 Ozturk, M., Altay, V., Gönenç, T. M., Unal, B. T., Efe, R., Akçiçek, E., & Bukhari, A. (2021).

914   An Overview of Olive Cultivation in Turkey: Botanical Features, Eco-Physiology and

915   Phytochemical Aspects. *Agronomy*, *11*(2), 295.

916   https://doi.org/10.3390/agronomy11020295

917 Patra, M., & Sharma, A. (2000). Mercury toxicity in plants. *The Botanical Review*, *66*(3), 379–

918   422. https://doi.org/10.1007/BF02868923

919 Pleijel, H., Klingberg, J., Nerentorp, M., Broberg, M. C., Nyirambangutse, B., Munthe, J., &

920   Wallin, G. (2021). *Mercury accumulation in leaves of different plant types – the*

921   *significance of tissue age and specific leaf area* [Preprint]. Biogeochemistry: Air - Land

922   Exchange. https://doi.org/10.5194/bg-2021-117

923 Pokharel, A. K., & Obrist, D. (2011). Fate of mercury in tree litter during decomposition.

924   *Biogeosciences*, *8*(9), 2507–2521. https://doi.org/10.5194/bg-8-2507-2011

925 Proietti, P., & Famiani, F. (2002). Diurnal and Seasonal Changes in Photosynthetic

926   Characteristics in Different Olive (Olea europaea L.) Cultivars. *Photosynthetica*, *40*(2),

927   171–176. https://doi.org/10.1023/A:1021329220613

928   Rea, A. W., Keeler, G. J., & Scherbatskoy, T. (1996). The deposition of mercury in throughfall

929   and litterfall in the lake champlain watershed: A short-term study. *Atmospheric*

930   *Environment*, *30*(19), 3257–3263. https://doi.org/10.1016/1352-2310(96)00087-8

931   Rea, A. W., Lindberg, S. E., Scherbatskoy, T., & Keeler, G. J. (2002). *Mercury Accumulation in*

932   *Foliage over Time in Two Northern Mixed-Hardwood Forests*. 19.

933   Riaz, M., Kamran, M., Fang, Y., Wang, Q., Cao, H., Yang, G., Deng, L., Wang, Y., Zhou, Y.,

934   Anastopoulos, I., & Wang, X. (2021). Arbuscular mycorrhizal fungi-induced mitigation

935   of heavy metal phytotoxicity in metal contaminated soils: A critical review. *Journal of*

936   *Hazardous Materials*, *402*, 123919. https://doi.org/10.1016/j.jhazmat.2020.123919

937   Richardson, J. B., Friedland, A. J., Engerbretson, T. R., Kaste, J. M., & Jackson, B. P. (2013).

938   Spatial and vertical distribution of mercury in upland forest soils across the northeastern

939   United States. *Environmental Pollution (Barking, Essex : 1987)*, *182*, 127–134.

940   https://doi.org/10.1016/j.envpol.2013.07.011

941   Sanz-Cortés, F., Martinez-Calvo, J., Badenes, M. L., Bleiholder, H., Hack, H., Llacer, G., &

942   Meier, U. (2002). Phenological growth stages of olive trees (Olea europaea). *Annals of*

943   *Applied Biology*, *140*(2), 151–157. https://doi.org/10.1111/j.1744-7348.2002.tb00167.x

944   Schaefer, K., Elshorbany, Y., Jafarov, E., Schuster, P. F., Striegl, R. G., Wickland, K. P., &

945   Sunderland, E. M. (2020). Potential impacts of mercury released from thawing

946   permafrost. *Nature Communications*, *11*(1), Article 1. https://doi.org/10.1038/s41467-

947   020-18398-5

948   Schneider, L., Allen, K., Walker, M., Morgan, C., & Haberle, S. (2019). Using Tree Rings to

949   Track Atmospheric Mercury Pollution in Australia: The Legacy of Mining in Tasmania.

950   *Environmental Science & Technology*, *53*(10), 5697–5706.

951   https://doi.org/10.1021/acs.est.8b06712

952   Schwesig, D., & Krebs, O. (2003). The role of ground vegetation in the uptake of mercury and

953   methylmercury in a forest ecosystem. *Plant and Soil*, 11.

954   Senesil, G. S., Baldassarre, G., Senesi, N., & Radina, B. (1999). Trace element inputs into soils

955   by anthropogenic activities and implications for human health. *Chemosphere*, *39*(2), 343–

956   377. https://doi.org/10.1016/S0045-6535(99)00115-0

957   Sghaier, A., Perttunen, J., Sievaènen, R., Boujnah, D., Ouessar, M., Ben Ayed, R., & Naggaz, K.

958   (2019). Photosynthetical activity modelisation of olive trees growing under drought

959   conditions. *Scientific Reports*, *9*(1), 15536. https://doi.org/10.1038/s41598-019-52094-9

960   Siudek, P., Kurzyca, I., & Siepak, J. (2016). Atmospheric deposition of mercury in central

961   Poland: Sources and seasonal trends. *Atmospheric Research*, *170*, 14–22.

962   https://doi.org/10.1016/j.atmosres.2015.11.004

963   Teixeira, D. C., Lacerda, L. D., & Silva-Filho, E. V. (2017). Mercury sequestration by

964   rainforests: The influence of microclimate and different successional stages.

965   *Chemosphere*, *168*, 1186–1193. https://doi.org/10.1016/j.chemosphere.2016.10.081

966   Terral, J.-F., Alonso, N., Capdevila, R. B. i, Chatti, N., Fabre, L., Fiorentino, G., Marinval, P.,

967   Jordá, G. P., Pradat, B., Rovira, N., & Alibert, P. (2004). Historical biogeography of olive

968   domestication (Olea europaea L.) as revealed by geometrical morphometry applied to

969   biological and archaeological material: Historical biogeography of olive domestication

970   (Olea europaea L.). *Journal of Biogeography*, *31*(1), 63–77.

971   https://doi.org/10.1046/j.0305-0270.2003.01019.x

972   Tomiyasu, T., Matsuo, T., Miyamoto, J., Imura, R., Anazawa, K., & Sakamoto, H. (2005). Low

973   level mercury uptake by plants from natural environments—Mercury distribution in

974   Solidago altissima L.-. *Environmental Sciences: An International Journal of*

975   *Environmental Physiology and Toxicology*, *12*(4), 231–238.

976   UNEP. (2019). *Technical Background Report to the Global Mercury Assessment 2018*. IVL

977   Svenska Miljöinstitutet.

978   Wang, X., Lin, C.-J., Lu, Z., Zhang, H., Zhang, Y., & Feng, X. (2016). Enhanced accumulation

979   and storage of mercury on subtropical evergreen forest floor: Implications on mercury

980   budget in global forest ecosystems: HG STORAGE ON SUBTROPICAL FOREST

981   FLOOR. *Journal of Geophysical Research: Biogeosciences*, *121*(8), 2096–2109.

982   https://doi.org/10.1002/2016JG003446

983   Wängberg, I., Munthe, J., Pirrone, N., Iverfeldt, Å., Bahlman, E., Costa, P., Ebinghaus, R., Feng,

984   X., Ferrara, R., Gårdfeldt, K., Kock, H., Lanzillotta, E., Mamane, Y., Mas, F., Melamed,

985   E., Osnat, Y., Prestbo, E., Sommar, J., Schmolke, S., … Tuncel, G. (2001). Atmospheric

986   mercury distribution in Northern Europe and in the Mediterranean region. *Atmospheric*

987   *Environment*, *35*(17), 3019–3025. https://doi.org/10.1016/S1352-2310(01)00105-4

988   Weigelt, A., Ebinghaus, R., Manning, A. J., Derwent, R. G., Simmonds, P. G., Spain, T. G.,

989   Jennings, S. G., & Slemr, F. (2015). Analysis and interpretation of 18 years of mercury

990   observations since 1996 at Mace Head, Ireland. *Atmospheric Environment*, *100*, 85–93.

991   https://doi.org/10.1016/j.atmosenv.2014.10.050

992   Wofsy, S. C., Goulden, M. L., Munger, J. W., Fan, S.-M., Bakwin, P. S., Daube, B. C., Bassow,

993   S. L., & Bazzaz, F. A. (1993). Net Exchange of CO_2 in a Mid-Latitude Forest. *Science*,

994   *260*(5112), 1314–1317. https://doi.org/10.1126/science.260.5112.1314

995   Wohlgemuth, L., Rautio, P., Ahrends, B., Russ, A., Vesterdal, L., Waldner, P., Timmermann, V.,

996   Eickenscheidt, N., Fürst, A., Greve, M., Roskams, P., Thimonier, A., Nicolas, M.,

997   Kowalska, A., Ingerslev, M., Merilä, P., Benham, S., Iacoban, C., Hoch, G., … Jiskra, M.

998   (2021). *Physiological and climate controls on foliar mercury uptake by European tree*

999   *species* [Preprint]. Biogeochemistry: Air - Land Exchange. https://doi.org/10.5194/bg-

1000   2021-239

1001   Wright, L. P., Zhang, L., & Marsik, F. J. (2016). Overview of mercury dry deposition, litterfall,

1002   and throughfall studies. *Atmospheric Chemistry and Physics*, *16*(21), 13399–13416.

1003   https://doi.org/10.5194/acp-16-13399-2016

1004   Wu, S., Zhang, X., Chen, B., Wu, Z., Li, T., Hu, Y., Sun, Y., & Wang, Y. (2016). Chromium

1005   immobilization by extraradical mycelium of arbuscular mycorrhiza contributes to plant

1006   chromium tolerance. *Environmental and Experimental Botany*, *122*, 10–18.

1007   https://doi.org/10.1016/j.envexpbot.2015.08.006

1008   Yammine, P., Kfoury, A., El-Khoury, B., Nouali, H., El-Nakat, H., Ledoux, F., Courcot, D., &

1009   Aboukaïs, A. (2010). A preliminary evaluation of the inorganic chemical composition of

1010   atmospheric tsp in the selaata region, north lebanon. *Lebanese Science Journal*, *11*(1), 18.

1011   Yanai, R. D., Yang, Y., Wild, A. D., Smith, K. T., & Driscoll, C. T. (2020). New Approaches to

1012   Understand Mercury in Trees: Radial and Longitudinal Patterns of Mercury in Tree Rings

1013   and Genetic Control of Mercury in Maple Sap. *Water, Air, & Soil Pollution*, *231*(5), 248.

1014   https://doi.org/10.1007/s11270-020-04601-2

1015   Yang, Y., Yanai, R. D., Driscoll, C. T., Montesdeoca, M., & Smith, K. T. (2018). Concentrations

1016   and content of mercury in bark, wood, and leaves in hardwoods and conifers in four

1017   forested sites in the northeastern USA. *PLOS ONE*, *13*(4), e0196293.

1018   https://doi.org/10.1371/journal.pone.0196293

1019   Yazbeck, E. B., Rizk, G. A., Hassoun, G., El-Khoury, R., & Geagea, L. (2018). *Ecological*

1020   *characterization of ancient olive trees in Lebanon- Bshaaleh area and their age*

1021   *estimation*. *11*(2 Ver. 1), 35–44.

1022   Zhao, X., & Wang, D. (2010). Mercury in some chemical fertilizers and the effect of calcium

1023   superphosphate on mercury uptake by corn seedlings (Zea mays L.). *Journal of*

1024   *Environmental Sciences*, *22*(8), 1184–1188. https://doi.org/10.1016/S1001-

1025   0742(09)60236-9

1026   Zhou, J., Obrist, D., Dastoor, A., Jiskra, M., & Ryjkov, A. (2021). Vegetation uptake of mercury

1027   and impacts on global cycling. *Nature Reviews Earth & Environment*, *2*(4), 269–284.

1028   https://doi.org/10.1038/s43017-021-00146-y

1029   Zhou, J., Wang, Z., & Zhang, X. (2018). Deposition and Fate of Mercury in Litterfall, Litter, and

1030   Soil in Coniferous and Broad-Leaved Forests. *Journal of Geophysical Research:*

1031   *Biogeosciences*, *123*(8), 2590–2603. https://doi.org/10.1029/2018JG004415

1032

1033
1034
1035
1036
1037
1038
1039

Supplementary Information

Table S1 Study sites geographic location and climatic data collected from the meteo stations installed by LARI.

Village Name	Location	Latitude (N)	Longitude (E)	Altitude (m a.s.l)	Temperature min-max (°C)	Annual mean Temperature (°C)	SD (±)	Annual mean rainfall (mm)	SD (±)
Bchaaleh	North Lebanon	34°12'06″	35°49'23″	1300	4-23	14	6.81	1631	110.17
Kawkaba	South Lebanon	33°23'85″	35°38'58″	672	7-27	17	6.76	1311	295.29

Table S2 Detailed synthesis of the Hg concentration values in different studies.

Table S2 in an Excel Format
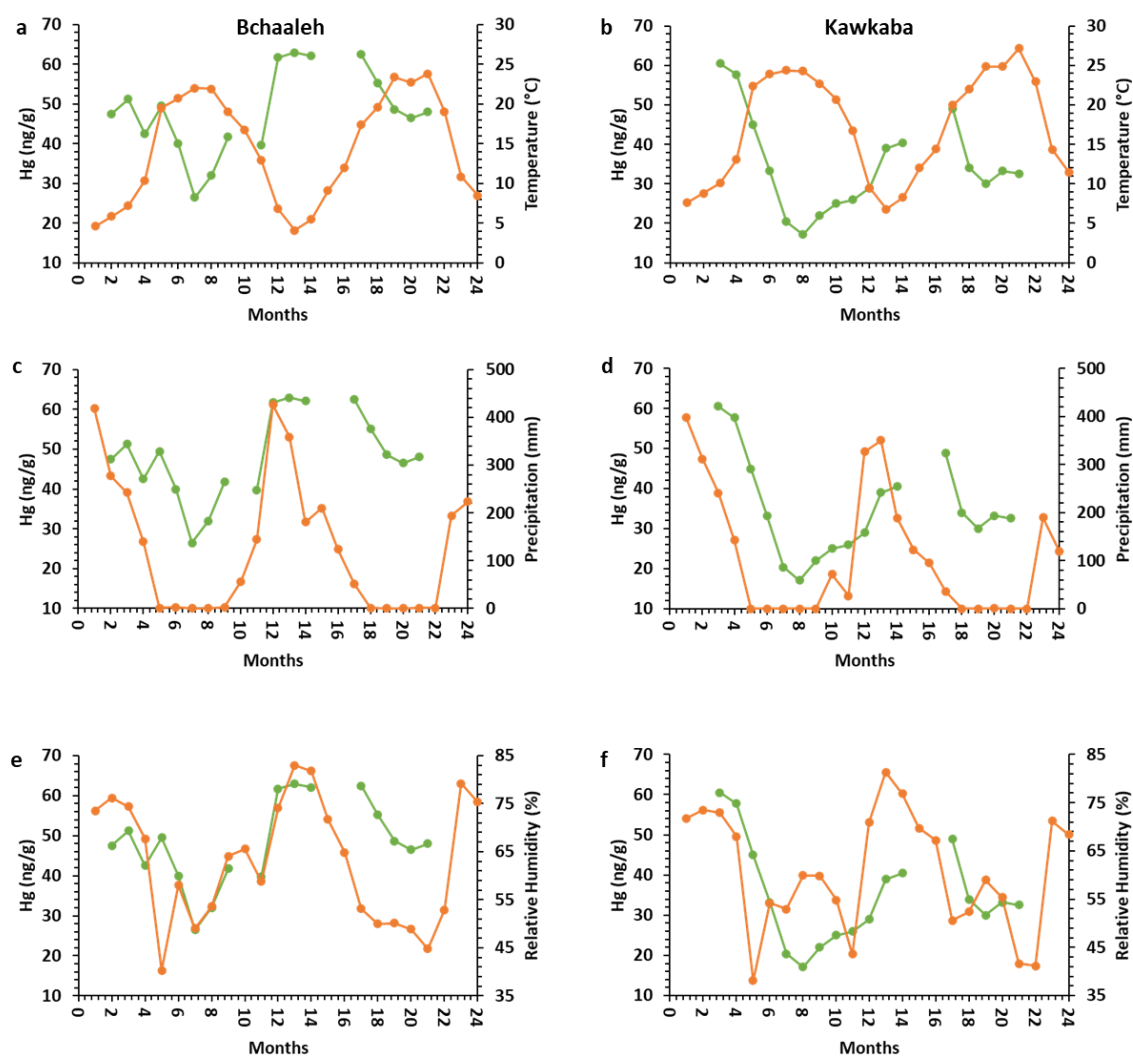
Fig. S1 Bchaaleh and Kawkaba (a) (b) Hg(ng/g) and Temperature(°C), (c) (d) Hg(ng/g) and Precipitation(mm) and (e) Hg(ng/g) and Relative Humidity (%).

Fig. S2 Map of Bchaaleh site and sampled tree locations. Upper terrace plot 2292 are under the endowment of the church. While Lower terrace plot 549 and 547 are a private property.

a
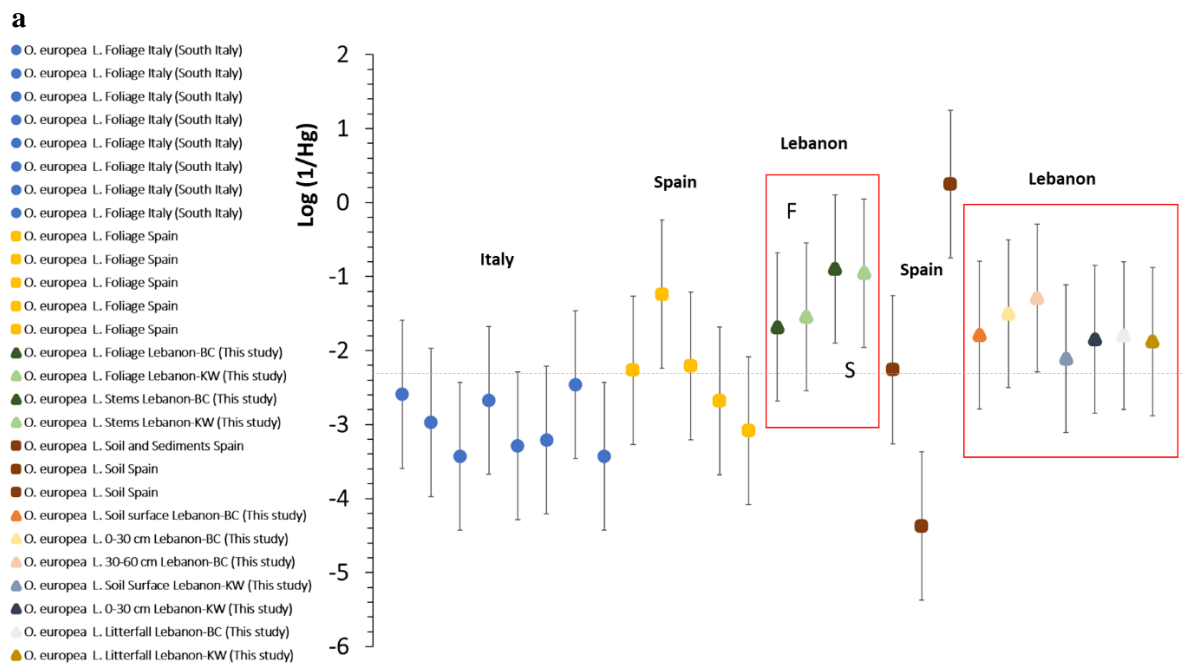
b
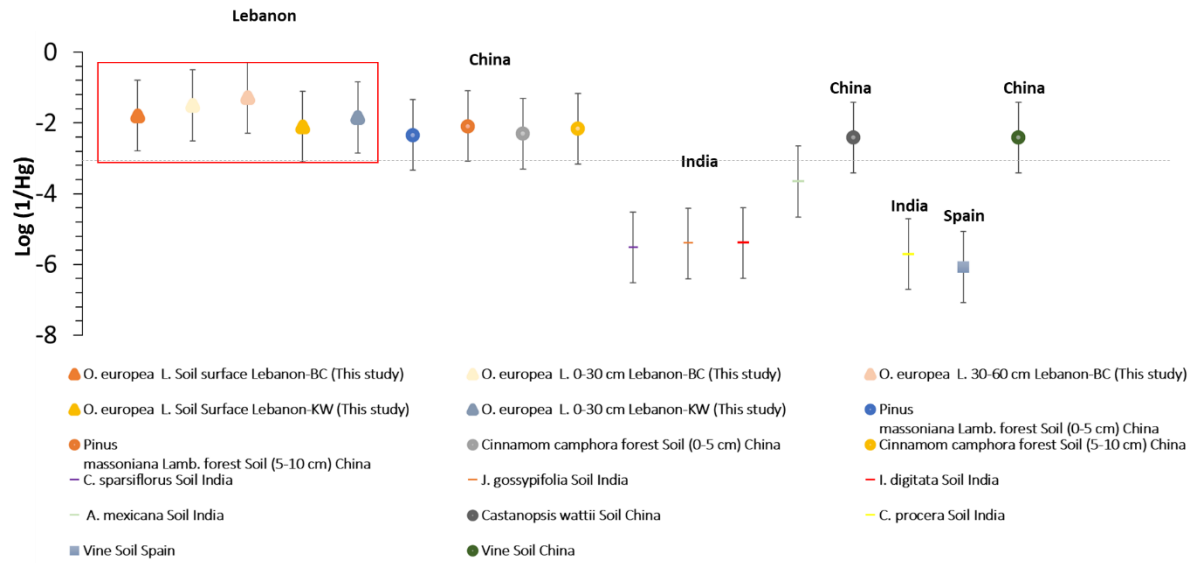
c
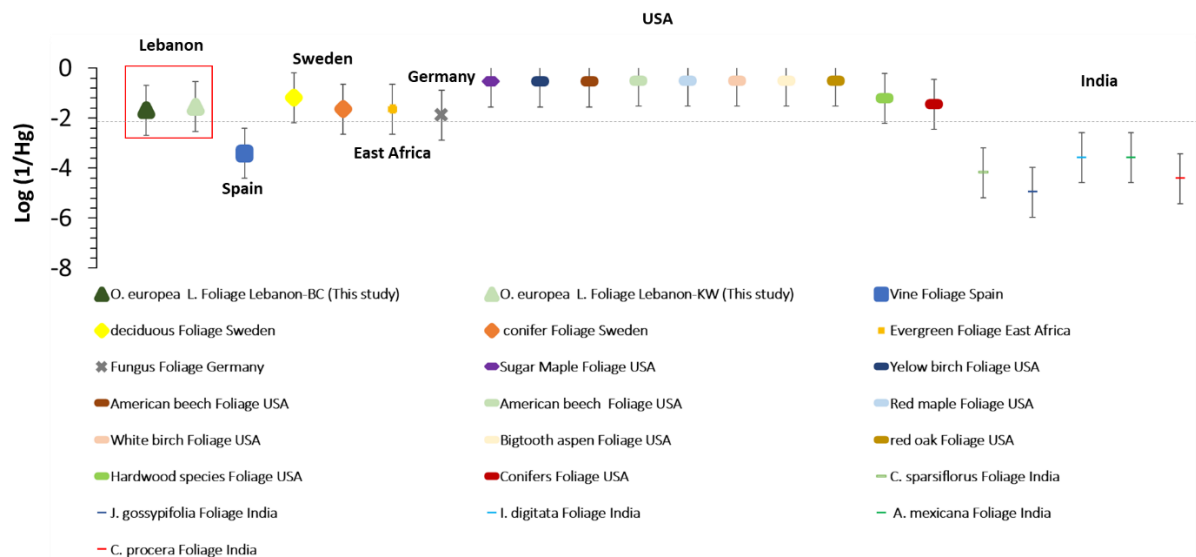
d
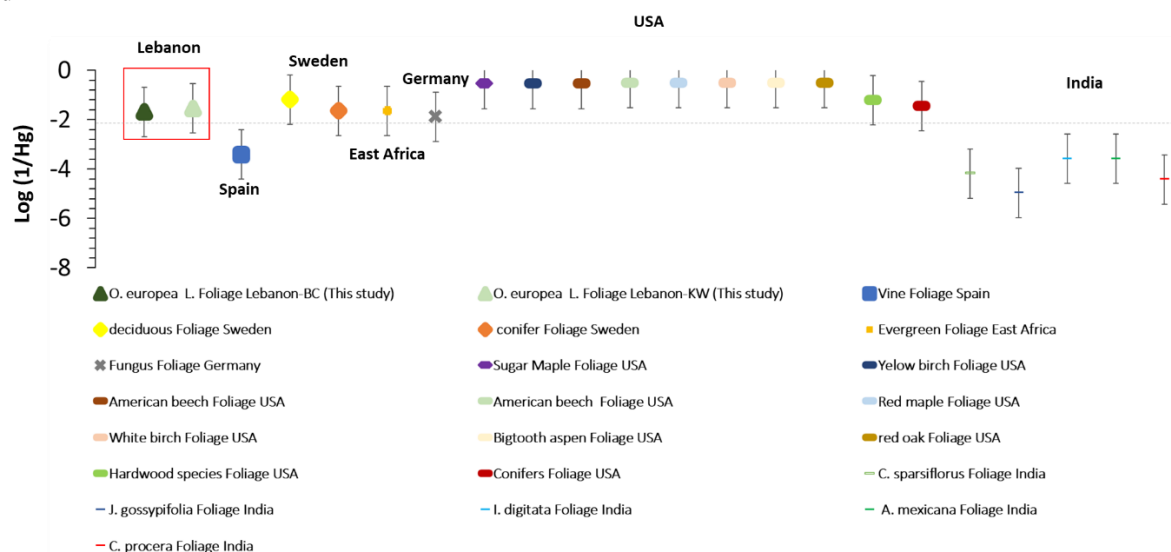
Fig. S3 Synthesis of Hg concentration for a) the Olive grove of the Mediterranean basin including foliage, stems, litter and soil. Our sites are indicated in red; b) the foliage of different species around the world; c) soil studies in different countries and d) litter, roots and stems of different species and countries. All the references are listed in Table S3. The gray dashed lines referrer to the threshold limit above which soil and plants are not contaminated.
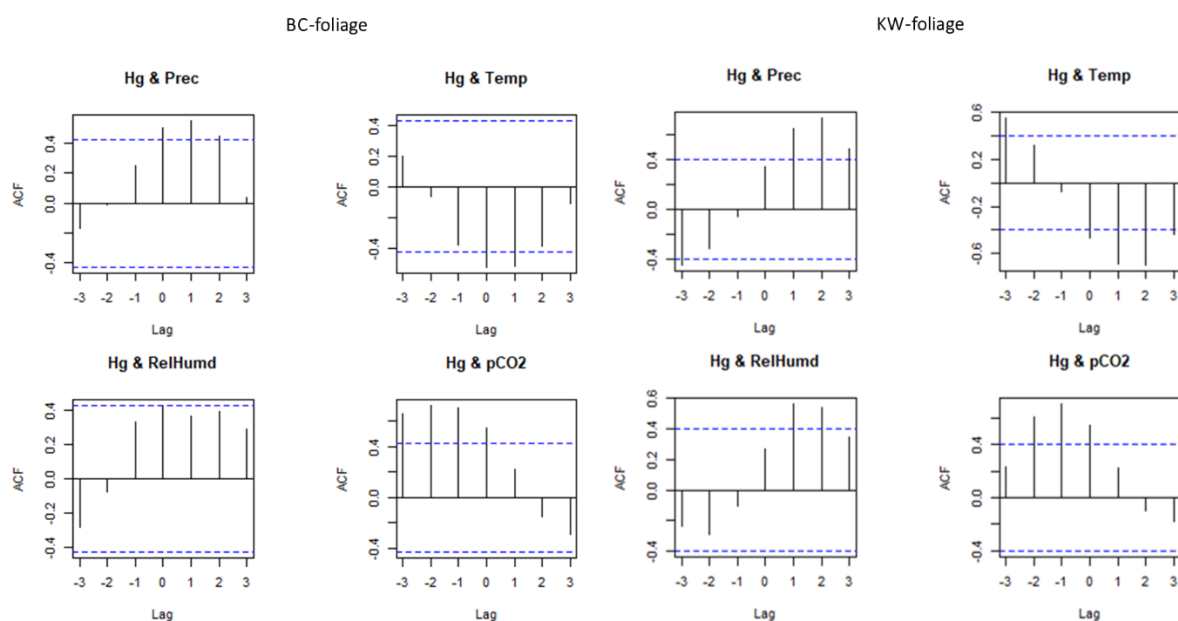
Fig. S4 Time lag test (R, Cross correlation) between the dependent variable (Hg) and the independent climatic variables in the foliage of BC and KW.

References for Supplementary Information

Amorós JA, Esbrí JM, García-Navarro FJ, Pérez-de-los-Reyes C, Bravo S, Villaseñor B, Higueras P (2014) Variations in mercury and other trace elements contents in soil and in vine leaves from the Almadén Hg-mining district. Journal of Soils and Sediments, 14(4), 773–777. https://doi.org/10.1007/s11368-013-0783-2

Bargagli R (1995) The elemental composition of vegetation and the possible incidence of soil contamination of samples. Science of The Total Environment, 176(1–3), 121–128. https://doi.org/10.1016/0048-9697(95)04838-3

Esbrí JM, López-Berdonces MA, Fernández-Calderón, S, Higueras P, Díez S (2015) Atmospheric mercury pollution around a chlor-alkali plant in Flix (NE Spain): An integrated analysis. Environmental Science and Pollution Research, 22(7), 4842–4850. https://doi.org/10.1007/s11356-014-3305-x

Fische RG, Rapsomanikis S, Andreae MO, Baldi F (1995) Bioaccumulation of methylmercury and transformation of inorganic mercury by macrofungi. Environmental Science & Technology 29(4), 993–999. https://doi.org/10.1021/es00004a020

Guarino F, Improta G, Triassi M, Castiglione S, Cicatelli A (2021) Air quality biomonitoring through *Olea europaea* L.: The study case of "Land of pyres." Chemosphere 282, 131052. https://doi.org/10.1016/j.chemosphere.2021.131052

Higueras P, Amorós JA, Esbrí JM, García-Navarro FJ, Pérez de los Reyes C, Moreno G (2012) Time and space variations in mercury and other trace element contents in olive tree leaves from the Almadén Hg-mining district. Journal of Geochemical Exploration 123, 143–151. https://doi.org/10.1016/j.gexplo.2012.04.012

Higueras P, Amorós, JÁ, Esbrí JM, Pérez-de-los-Reyes C, López-Berdonces MA, García-Navarro FJ (2016) Mercury transfer from soil to olive trees. A comparison of three different contaminated sites. Environmental Science and Pollution Research 23(7), 6055–6061. https://doi.org/10.1007/s11356-015-4357-2

Kabata-Pendias A and Pendias H (2000) Trace elements in soils and plants (3rd ed) CRC Press

Llanos W, Kocman D, Higueras P, Horvat M (2011) Mercury emission and dispersion models from soils contaminated by cinnabar mining and metallurgy. Journal of Environmental Monitoring 13(12), 3460. https://doi.org/10.1039/c1em10694e

Naharro R, Esbri J, Amorós J, Higueras P (2018) Atmospheric mercury uptake and desorption from olive-tree leaves. 20(EGU2018-2982,2018), 2

Pleijel H, Klingberg J, Nerentorp M, Broberg MC, Nyirambangutse B, Munthe J, Wallin G (2021) Mercury accumulation in leaves of different plant types – the significance of tissue age and specific leaf area [Preprint]. Biogeochemistry: Air - Land Exchange. https://doi.org/10.5194/bg-2021-117

Rea AW, Lindberg SE, Scherbatskoy T, Keeler GJ (2002) Mercury accumulation in foliage over time in two Northern mixed-hardwood forests. Water, Air, and Soil Pollution 133(1), 49-67

Senesil GS, Baldassarre G, Senesi N, Radina B (1999) Trace element inputs into soils by anthropogenic activities and implications for human health. Chemosphere 39(2), 343–377. https://doi.org/10.1016/S0045-6535(99)00115-0

Shaw BP and Panigrahi AK (1986) Uptake and tissue distribution of mercury in some plant species collected from a contaminated area in India: Its ecological implications. Archives of Environmental Contamination and Toxicology 15(4), 439–446. https://doi.org/10.1007/BF01066412

Teixeira DC, Lacerda LD, Silva-Filho EV (2017) Mercury sequestration by rainforests: The influence of microclimate and different successional stages. Chemosphere, 168:1186–1193. https://doi.org/10.1016/j.chemosphere.2016.10.081

Wang X, Li CJ, Lu Z, Zhang H, Zhang Y, Feng X (2016) Enhanced accumulation and storage of mercury on subtropical evergreen forest floor: Implications on mercury budget in global forest ecosystems: Hg storage on subtropical forest floor. Journal of Geophysical Research: Biogeosciences 121: 2096–2109. https://doi.org/10.1002/2016JG003446

Yang Y, Yanai RD, Driscoll CT, Montesdeoca M, Smith KT (2018) Concentrations and content of mercury in bark, wood, and leaves in hardwoods and conifers in four forested sites in the Northeastern USA. PLOS ONE 13(4): e0196293. https://doi.org/10.1371/journal.pone.0196293